JACS
JOURNAL OF THE AMERICAN CHEMICAL SOCIETY

Article

pubs.acs.org/JACS

C-Functionalized, Air- and Water-Stable 9,10-Dihydro-9,10-diboraanthracenes: Efficient Blue to Red Emitting Luminophores

Christian Reus, Sabine Weidlich, Michael Bolte, Hans-Wolfram Lerner, and Matthias Wagner*

Institut für Anorganische und Analytische Chemie, J. W. Goethe-Universität Frankfurt, Max-von-Laue-Straße 7, D-60438 Frankfurt (Main), Germany

Supporting Information

ABSTRACT: 9,10-Dihydro-9,10-diboraanthracene (DBA) provides a versatile scaffold for the development of boron-doped organic luminophores. Symmetrically C-halogenated DBAs are obtained through the condensation of 4-bromo-1,2-bis(trimethylsilyl)benzene or 4,5-dichloro-1,2-bis(trimethylsilyl)benzene with BBr_3 in hexane. Unsymmetrically C-halogenated DBAs are formed via an electrophilic solvent activation reaction if the synthesis is carried out in *o*-xylene. Mechanistic insight has been achieved by in situ NMR spectroscopy, which revealed C-halogenated 1,2-bis(dibromoboryl)benzenes to be the key intermediates. Treatment of the primary 9,10-dibromo-DBAs with MesMgBr yields air- and water-stable C-halogenated 9,10-dimesityl-DBAs (2-Br-6,7-Me_2-DBA$(Mes)_2$; 2,6-Br_2-DBA$(Mes)_2$; 2,3-Cl_2-6,7-Me_2-DBA$(Mes)_2$; 2,3,6,7-Cl_4-DBA$(Mes)_2$). Subsequent Stille-type C−C-coupling reactions give access to corresponding phenyl, 2-thienyl, and *p*-*N*,*N*-diphenylaminophenyl derivatives, which act as highly emissive donor−acceptor dyads or donor−acceptor−donor triads both in solution and in the solid state. 2-Thienyl was chosen as a model substituent to show that already a variation of the number and/or the positional distribution of the donor groups suffices to tune the emission wavelength of the resulting benchtop stable compounds from 469 nm (blue) to 540 nm (green). A further shift of the fluorescence maximum to 594 nm (red) can be achieved by switching from 2-thienyl to *p*-aminophenyl groups. A comparison of the optoelectronic properties of selected C-substituted DBA$(Mes)_2$ derivatives with those of the isostructural anthracene analogues unveiled the following: (i) The DBA core is a much better electron acceptor. (ii) The emission colors of DBAs fall in the visible range of the spectrum (blue to orange), while anthracenes emit exclusively in the near-ultraviolet to blue wavelength regime. (iii) DBAs show significantly higher solid-state quantum yields.

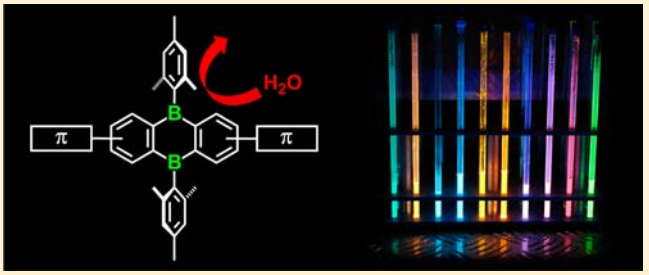

INTRODUCTION

Carbon-based π-conjugated systems nowadays represent an important class of materials with applications in a wide range of contemporary technological areas[1] such as organic electronics,[2,3] light-emitting devices,[4] or photovoltaics.[5] Low-cost organic materials exhibit advantageous properties such as being lightweight, high mechanical flexibility, and solution processability, which are not found in their silicon or metal counterparts. However, purely organic compounds with small band gaps and/or low-lying LUMO energies are rare and often suffer from distinct disadvantages (cf., pentacene is O_2-sensitive[6] and prone to dimerization via Diels−Alder reactions[7]).[8] The replacement of selected carbon atoms within the organic π system by main-group heteroatoms like B,[9] Si,[10] N,[11] P,[12] or S[13] has been used as a tool to circumvent these shortcomings and, moreover, ever since has emerged as a powerful method to open exciting new possibilities. Especially the implementation of Lewis acidic boron atoms has proven to result in very desirable optoelectronic properties such as high electron affinities (leading to n-type materials) and intense luminescence.[9] These effects are rooted in the interaction of the vacant p orbital at the boron center with the surrounding π-electron clouds, which is particularly efficient in the molecules' LUMOs and thereby lowers the energies of these orbitals.

During the past five years, 9,10-dihydro-9,10-diboraanthracene (DBA) has been established as a promising building block for organic π-conjugated materials.[14−25] Because both 9,10-dibromo-9,10-dihydro-9,10-diboraanthracene (DBA$(Br)_2$)[19] and the parent compound DBA$(H)_2$[14] are readily available, a variety of 9,10-diorganyl-9,10-dihydro-9,10-diboraanthracene derivatives (DBA$(R)_2$, **A**; Figure 1) can be conveniently prepared through nucleophilic substitution or hydroboration reactions. Thus, in this approach, the unique chemical nature of the boron atom is exploited in two ways: Boron first serves as an expedient anchor group to facilitate the introduction of substituents into the molecule and afterward governs the electronic structure of the overall π-electron system. Using the 9,10-positions as the sole sites for derivatization, it has so far been possible not only to tune the emission characteristics of DBAs over a wide range, but also to prepare polymeric species[14,15] along with low-molecular weight compounds.

Despite these numerous positive aspects of **A**-type materials, two major drawbacks have to be overcome before applications of DBA fluorophores can be taken into serious consideration.

Received: July 3, 2013
Published: July 30, 2013

   dx.doi.org/10.1021/ja406766e | J. Am. Chem. Soc. 2013, 135, 12892−12907

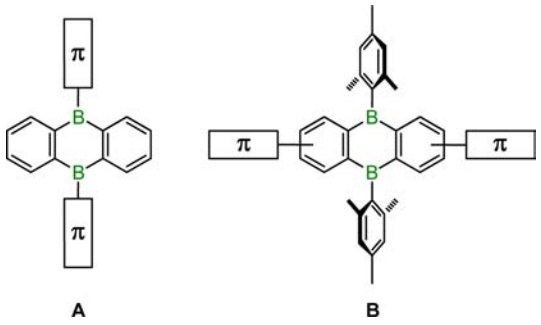

Figure 1. The B- and C-functionalized 9,10-dihydro-9,10-diboraanthracenes.

On the one hand, the quantum yields obtained so far rarely exceed 30%,[23] and, even more importantly, most DBA derivatives developed to date proved to be highly sensitive toward air and moisture. Usually, the weak links are the exocyclic B−C bonds, whereas the actual DBA framework tends to be rather stable (we commonly find the borinic acid $DBA(OH)_2$[19] as the product of hydrolytic degradation). The design of more inert DBAs has therefore to focus on the steric shielding of the vacant boron p orbital and on the kinetic protection of the exocyclic B−C bond.

Along these lines, 9,10-dimesityl-9,10-dihydro-9,10-diboraanthracene ($DBA(Mes)_2$) is a rare example of a long-term benchtop stable DBA derivative,[18,25] which we therefore selected as the lead structure for further materials development. $DBA(Mes)_2$ undergoes two reversible one-electron transitions at comparatively anodic redox potentials of $E_{1/2}$ = −1.84 V, −2.73 V (THF; vs FcH/FcH^+) and is thus electrochemically well behaved.[25] In C_6H_6, the compound fluoresces at 460 nm, yet with a low quantum efficiency of only 3%.[25] In contrast to **A**-type materials, the boron atoms of $DBA(Mes)_2$ are no longer available for further functionalization. As a consequence, any substituents have now to be introduced into the *o*-phenylene rings to create **B**-type materials (C-substitution; Figure 1). The successful application of such an approach to the synthesis of compounds with remarkable and useful optoelectronic properties has already been demonstrated for phenylene-functionalized dibenzoboroles[26] and dibenzo[*b*,*f*]borepins.[27] In the case of 9,10-dihydro-9,10-diboraanthracenes, however, corresponding examples are restricted to three frameworks: perfluorinated DBAs,[28] 6,13-dihydro-6,13-diborapentacenes,[29,30] and a DBA-containing graphene flake.[24] The scarcity of C-substituted DBAs has to be attributed to the lack of appropriately substituted 1,2-bis(trimethylsilyl)benzenes, which generally serve as the key starting materials in DBA syntheses.

Very recently, our group reported viable routes to various halogenated 1,2-bis(trimethylsilyl)benzenes,[31,32] which now puts us into the position to prepare C-halogenated DBAs. In this context, we have elucidated key intermediates and mechanistic details of the reaction sequence leading to the assembly of the $DBA(Br)_2$ framework. These investigations also resulted in the discovery of a unique C−H activation reaction of aromatic solvents, which gives access to unsymmetrically C-substituted DBAs in preparatively useful yields. C-Halogenated $DBA(Mes)_2$ derivatives provide a universal platform for further transformations, as the primary halogeno substituents can be replaced at will by organyl groups through Pd-mediated C−C-coupling reactions. Herein, we will prove the viability of this concept for the preparation of highly emissive (quantum yields up to 72%), air- and water-stable donor−acceptor−donor triads and donor−acceptor dyads. Appropriate choice of substituents allows a tuning of the emission colors from the blue to the red region of the visible-light spectrum. In the final part of this Article, we will directly compare selected DBA-containing species with their all-carbon anthracene analogues and show that boron doping significantly improves the materials' optoelectronic properties.

RESULTS AND DISCUSSION

Synthesis of Halogenated 9,10-Dimesityl-9,10-dihydro-9,10-diboraanthracenes. A convenient synthesis route to parent 9,10-dimesityl-9,10-dihydro-9,10-diboraanthracene ($DBA(Mes)_2$, R = H; **2**) starts from 1,2-bis(trimethylsilyl)-benzene (R = H; **1**)[31] and BBr_3, and is conducted in toluene solution at 120 °C in a sealed glass ampule (Scheme 1).[19] Subsequent

Scheme 1. Synthesis of Parent $DBA(Mes)_2$ (2; R = H)

1: R = H **2**: R = H

treatment of the intermediate $DBA(Br)_2$with MesMgBr provides **2** in an overall yield of 40%.[25] Given the comparatively high reaction temperature, the use of a very Lewis acidic boron halide and a strongly nucleophilic Grignard reagent, the selection of substituents R that are compatible with these conditions is rather limited. Halogen atoms are among the most promising candidates R, because they allow the introduction of a broad variety of organic substituents through Pd-catalyzed C−C-coupling reactions. The most readily available halogenated 1,2-bis(trimethylsilyl)benzenes are the compounds 4-fluoro- and 4-chloro-1,2-bis(trimethylsilyl)benzene,[31] as well as 4-bromo- (**3**)[32] and 3,4-dichloro-1,2-bis(trimethylsilyl)benzene (**4**),[31] which are shown in Scheme 2. For our purposes, **3** appeared to be best suited, because C−Br bonds are usually easier to activate than C−F/Cl bonds. Because the 4,5-dibrominated 1,2-bis(trimethylsilyl)benzene is unknown, we included the corresponding 4,5-dichloro-1,2-bis(trimethylsilyl)benzene (**4**; Scheme 2) in our investigation.

Our first syntheses of halogenated $DBA(Mes)_2$ species employing **3** and **4** relied on the protocol developed for the preparation of pristine **2** (Scheme 1). After workup, we noted two unexpected results: (i) The ratio between the two isomeric products 2,6-Br_2-$DBA(Mes)_2$ (**5**) and 2,7-Br_2-$DBA(Mes)_2$ (**6**) was not 1:1 but 3:2. (ii) With both starting materials **3** and **4**, the target compounds **5**/**6** and **10** were the minor constituents in the product mixture; as major constituents, we identified the unsymmetrically substituted DBAs **7**/**8** and **12**, which had obviously formed through solvent (toluene) activation (Scheme 2).

Given this background, we performed a systematic screening of reaction temperature profiles and solvents and come to the conclusion that the optimum conditions are dependent on the desired product specifications:

(1) If the focus lies on a maximum overall yield of **5**/**6** or **10**, the DBA scaffold should be assembled under the following conditions: hexane, 120 °C, sealed glass ampule, 1.5 d (Scheme 2). As a drawback, this procedure does not discriminate at all between **5** and **6**, but leads to a 1:1 mixture.

dx.doi.org/10.1021/ja406766e | J. Am. Chem. Soc. 2013, 135, 12892−12907

Scheme 2. Synthesis of the Halogenated DBA(Mes)$_2$ Derivatives 5−13[a]

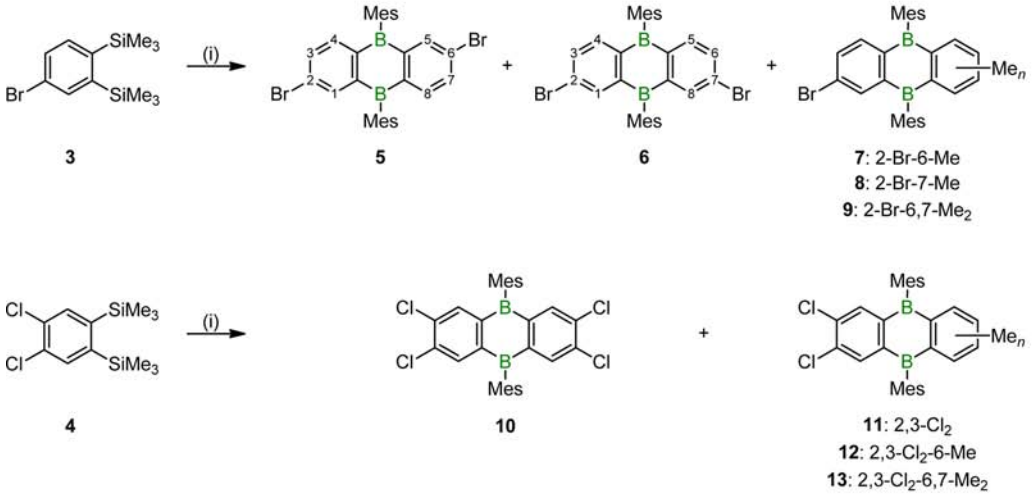

	product ratio			
	hex	C_6H_6	tol	o-xyl[a]
5	1	3	3	3
6	1	2	2	2
7/8	-	-	7	-
9	-	-	-	10
Yield	43%	31%	32%	33%
10	1	1	1	1
11	-	1.4	-	-
12	-	-	2	-
13	-	-	-	7
Yield	60%	38%	31%	34%

[a]The table shows the overall yield over the two-step reaction and the proportion of the solvent-activated products **7**−**9** and **11**−**13** (n = 0−2), respectively. (i) (1) +BBr_3 (3 equiv), 120 °C, 36 h, solvent as indicated in the table; (2) removal of all volatiles, +MesMgBr (2 equiv in THF), toluene, 0 °C, 12 h. (a) A 1:1 mixture hexane:*o*-xylene was used.

(2) If the discrimination between **5** and **6** is the main issue, the reaction should be carried out in C_6H_6 instead of hexane (Scheme 2).

(3) If the amount of unsymmetrically substituted DBAs is to be maximized, a 1:1 mixture of hexane with the electron-rich *o*-xylene is a particularly reactive solvent, which, contrary to toluene, generates exclusively one monobromo derivative **9** (Scheme 2).

In all cases, best yields were obtained when the air- and moisture-sensitive halogenated DBA(Br)$_2$ intermediates were directly converted to the air- and water-stable mesitylated target products without prior purification. We also note that the yield of the parent compound DBA(Mes)$_2$ (**2**; R = H) improves considerably if hexane is used instead of toluene[19] as solvent in the first step of the synthesis sequence.

With the aim to learn more about the factors governing the formation of the isomer 2,6-Br$_2$-DBA(Mes)$_2$ (**5**) versus 2,7-Br$_2$-DBA(Mes)$_2$ (**6**), we monitored the reaction between **3** and BBr_3 by NMR spectroscopy. Three key factors were varied: (i) the amount of BBr_3 (substoichiometric 0.35 equiv and the regular 3 equiv), (ii) the solvent (perdeuterated cyclohexane (C_6D_{12}) and C_6D_6), and (iii) the reaction temperature (room temperature and 120 °C).

The room-temperature data are discussed first. In C_6D_{12}, **3** and BBr_3 showed no reaction within 1 d, irrespective of the amount of BBr_3 employed.[33] A significantly different result was obtained for the C_6D_6 samples: Addition of 0.35 equiv of BBr_3 to **3** essentially gave a mixture of the starting materials and 4-bromo-1-dibromoboryl-2-trimethylsilylbenzene **14** after 1 d (Scheme 3; cf., the Supporting Information for more details).[33] The qualitative picture did not change when the amount of BBr_3 was raised to 3 equiv, but the ratio **3**:**14** inverted from 6:1 to 1:6 (1 d); the conversion to **14** was quantitative after 2 d. Most importantly, we found no indication for the formation of the other possible isomer 4-bromo-2-dibromoboryl-1-trimethylsilylbenzene. Thus, at room temperature, the Si/B exchange proceeds selectively para to the bromine atom, as to be expected from the strongly ortho/para directing effect of a bromo substituent in electrophilic aromatic substitution

Scheme 3. Mechanistic Investigation into the Reaction of 3 with BBr_3 and Proposed Reaction Mechanism for the Assembly of the DBA Scaffold via the Main Intermediate 14[a]

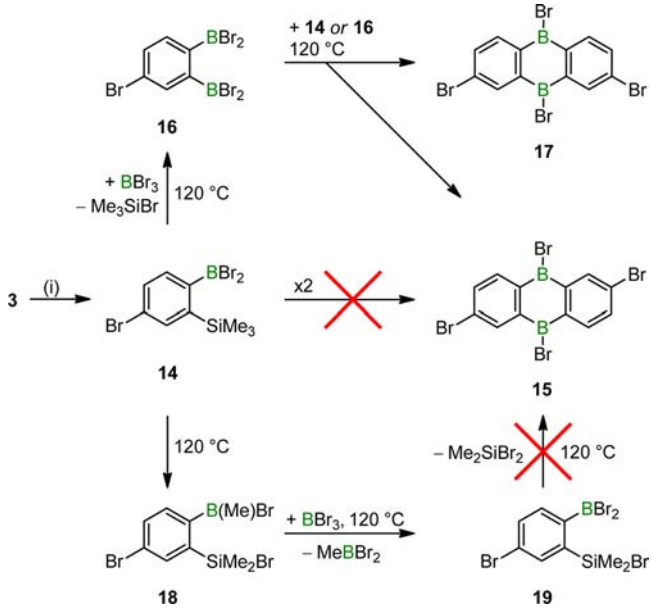

[a]Bottom: Br/Me rearrangement reaction of **14** leading to the side products **18** and **19**. (i) +BBr_3 (0.35 or 3 equiv); C_6D_6, room temperature (quantitative after 2 d) or C_6D_{12}, 120 °C.

reactions.[34] Moreover, the introduction of a first BBr_2 group apparently deactivates the aromatic system to such an extent that a second Si/B exchange does not take place under ambient conditions.[35] This explains why neither 4-bromo-1,2-bis-(dibromoboryl)benzene **16** nor dibrominated DBA(Br)$_2$ (**15**/**17**) could be observed in the room-temperature experiments.

The results described in the following for experiments carried out at 120 °C equally apply for the C_6D_{12} and the C_6D_6 samples. The reaction of **3** with 0.35 equiv of BBr_3 completely consumed the BBr_3 during 1 d and yielded **14** together with

dx.doi.org/10.1021/ja406766e | J. Am. Chem. Soc. 2013, 135, 12892−12907

dibrominated DBA(Br)$_2$ (**15**/**17**). Further heating of the sample mainly led to a rearrangement of **14** into **18**.[36] When using 3 equiv of BBr_3, **15**/**17** started to precipitate after 2 h, and a solution containing **14**, **18**, and 4-bromo-1-dibromoboryl-2-bromodimethylsilylbenzene (**19**) was obtained.

After 1 d, only **18** and **19** had remained in the solution; more prolonged reaction times led to a gradual decrease of the relative amount of **18** and to a concomitant increase in the concentration of **19**. **19** is thus likely generated through the reaction of **18** with BBr_3 (signals of the byproduct $MeBBr_2$ also appeared in the NMR spectra).

After mesitylation of the obtained **15**/**17**, ^{1}H NMR spectroscopy indicated isomer distributions of **5**:**6** = 1:1 (C_6D_{12}) and 3:2 (C_6D_6). The only experimentally established B/Si-substituted bromobenzene was **14**; resonances of its isomer 4-bromo-1-dibromoboryl-2-bromodimethylsilylbenzene never occurred in the NMR spectra. If **15**/**17** were solely formed through the homodimerization of **14**, one would consequently expect perfect selectivity for the isomer 2,6-Br_2-DBA(Br)$_2$ (**15**) in the present case. The total lack of selectivity in C_6D_{12} and the moderate selectivity in C_6D_6 solution therefore point toward a B/Si-exchange on **14** at elevated temperatures furnishing the 1,2-diborylated benzene **16**. The more symmetrical compound **16** will react with itself or **14** in a less discriminative fashion regarding the formation of either **15** or **17**. Indeed, during our high-temperature NMR-monitoring studies with excess BBr_3, we came across one set of signals not mentioned so far, which we tentatively assign to **16** (Scheme 3; cf., the Supporting Information for more details).

To test this working hypothesis, we first heated a solution of pure **14** in C_6D_6 to 120 °C for extended periods of time. As a result, extensive Br/Me rearrangement (**14**→**18**) but no formation of **15**/**17** took place. The experiment was next repeated in the presence of a catalytic amount of BBr_3 (approximately 5 mol %). This time, the reaction gave **18** in addition to **15**/**17**; however, the DBA assembly was slowed, and the yield of **15**/**17** was markedly lower than usual. Importantly, the isomer ratio determined after mesitylation of **15**/**17** was again 3:2, thereby confirming the adverse effect of the likely key intermediate **16** on the isomer selectivity **15** versus **17** (Scheme 3).

Our mechanistic investigations not only shed light on the factors governing the isomer distribution **15**/**17**, but also clarify why the combined yields of **5**/**6** never exceeded 60%. After the usual heating time of 1−1.5 d, the product mixture resulting from **3** and BBr_3 contained **15**/**17**, **18**, and **19** irrespective of the solvent employed. Longer heating times did not effect a decrease in the concentration of **19**. Moreover, we detected only negligible quantities of Me_2SiBr_2 as compared to the amount of Me_3SiBr present in the solution. Contrary to the $SiMe_3$ group, the Si(Br)Me_2 substituent apparently does not take part in further B/Si exchange processes, which is why **18** and **19** represent dead ends of the **15**/**17** synthesis sequence. In agreement with the fact that the Si−Ph bond cleavage by BBr_3 is less facile in C_6D_{12} than in C_6D_6, we also monitored a much lower relative content of **19** in heated C_6D_{12} than in heated C_6D_6, which explains the generally better yields of 9,10-dihydro-9,10-diboraanthracene syntheses in hexane as compared to aromatic solvents. Moreover, the reaction **14**→**15**/**17** requires BBr_3 as a catalyst (to generate **16** as key intermediate), while the rearrangement **14**→**18** is essentially independent of the BBr_3 concentration. The use of excess BBr_3 (i.e., 3 equiv per molecule **3**) consequently improves the yields of **15**/**17** (relative to **18**) by accelerating the desired one of the two competing reaction pathways.

With respect to the solvent-activation reaction, the following trends are worth mentioning: (i) The nonhalogenated bis(trimethylsilyl)benzene **1** neither reacts with C_6H_6, nor with toluene, nor with *o*-xylene; (ii) the monobrominated derivative **3** is inert toward C_6H_6 but activates toluene and, to an even greater extent, *o*-xylene; and (iii) the dichlorinated derivative **4** reacts even with C_6H_6 but again gives best results with *o*-xylene (cf., **10**:**13** = 1:7; Scheme 2). Highest yields of an unsymmetrically substituted DBA(Mes)$_2$ are thus obtained when an electron-poor 1,2-bis(trimethylsilyl)benzene is combined with an electron-rich aromatic solvent. It is worth mentioning that the solvent activation mechanism necessarily involves the liberation of HBr, which, in turn, can induce unwanted protodesilylation processes (cf., ref 33) and thereby lower the product yields.

Our current working hypothesis is that the solvent activation step proceeds through electrophilic aromatic borylation, which requires electron-deficient boron reagents. 1,2-Diborylbenzenes are already strong Lewis acids, and the introduction of halogen atoms into the phenylene ring should further enhance their Lewis acidity (cf., **16**; Scheme 3). However, the best established aromatic borylation mechanisms involve boron cations as key intermediates.[37] We therefore assume that the solvent activation process has to be promoted by bromide abstraction from the reacting boron center, which could be achieved either by attack of external BBr_3[38] or by the formation of an intramolecular B−Br···B acid−base adduct (Figure 2, left). A related

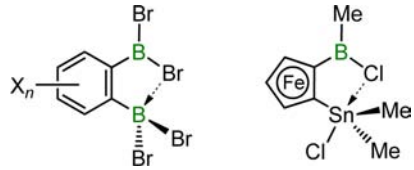

Figure 2. Left: Intramolecular B−Br···B adduct as the proposed intermediate of the electrophilic aromatic solvent borylation reaction (X = Br, *n* = 1; X = Cl, *n* = 2). Right: Structurally characterized ferrocene-based bidentate B/Sn Lewis acid forming an intramolecular B−Cl···Sn adduct.[39]

intramolecular B−Cl···Sn adduct has been characterized by X-ray crystallography for ferrocene-based bidentate B/Sn Lewis acids (Figure 2, right).[39]

All compounds **5**−**13** compiled in Scheme 2 have been synthesized on a preparative scale and employed in further reactions (see below). A comparison of the key optoelectronic parameters of the toluene-derived DBA(Mes)$_2$ species with those of the *o*-xylene-derived ones revealed no significant differences. From now on, toluene-derived compounds will therefore be excluded from detailed discussions.

The dibrominated DBA(Mes)$_2$ was obtained as an analytically pure pair of isomers **5**/**6** in yields of 43% (hexane; **5**:**6** = 1:1) or 31% (C_6H_6; **5**:**6** = 3:2) based on **3**. The two isomers could not be separated from each other, even by HPLC. However, after substitution of bromine atoms for, e.g., 2-thienyl groups, chromatographic separation was possible (cf., compounds **23**/**24** below). The tetrachlorinated DBA(Mes)$_2$ **10** is readily accessible in 60% overall yield. Even though all of the solvent-activated compounds are inevitably contaminated with the corresponding symmetrically substituted DBA(Mes)$_2$

dx.doi.org/10.1021/ja406766e | J. Am. Chem. Soc. 2013, 135, 12892−12907

species, an almost quantitative enrichment can be achieved by (repeated) HPLC. It is yet more convenient to use the mixtures for subsequent C−C-coupling reactions and to perform the separation step afterward by conventional column chromatography.

Similar to pristine **2**, the halogeno derivatives are air- and moisture-stable both in solution and in the solid state for extended periods of time. **5**−**13** are soluble in aromatic solvents, but they dissolve better in chlorinated hydrocarbons; NMR data were therefore recorded in $CDCl_3$ (cf., the Supporting Information for plots of all spectra).

The $^{11}B\{^1H\}$ NMR spectra of all $DBA(Mes)_2$ derivatives **5**−**13** are characterized by very broad resonances in the range 69−74 ppm (cf., **2**: $\delta(^{11}B) = 66$[18]). 2,6-Br_2-$DBA(Mes)_2$ (**5**) can easily be distinguished from 2,7-Br_2-$DBA(Mes)_2$ (**6**) in the ^1H NMR spectrum, because it gives rise to only one set of mesityl resonances, whereas two sets appear in the spectrum of **6**. Both in **5** and in **6**, the *o*-phenylene protons give rise to one small doublet ($^4J_{HH}$ coupling), one large doublet ($^3J_{HH}$ coupling), and one doublet of doublets; corresponding signals possess only marginally different chemical shift values in both isomers. Because of its high symmetry, Cl_4-$DBA(Mes)_2$ (**10**) exhibits only one singlet proton resonance for the DBA backbone. In the cases of the unsymmetrically substituted $DBA(Mes)_2$ derivatives, the general NMR features of the halogenated *o*-phenylene rings remain essentially the same as in **5**/**6** or **10**. The *o*-phenylene fragment in **11** gives rise to two multiplets in the ^1H NMR spectrum, reminiscent of the parent compound **2**. The *o*-xylene-derived species **13** shows one C*H* and one C*CH*$_3$ resonance, while symmetry reduction in **9** leads to two aromatic C*H* signals (the two C*CH*$_3$ resonances are overlapping).

The molecular structures of **5** and **10** were determined by X-ray crystallography (Figure 3; cf., the Supporting Information for the X-ray crystal structure analysis of Cl_4-$DBA(Br)_2$). In both centrosymmetric compounds, the planes of the mesityl substituents are almost perpendicular to the DBA plane with dihedral angles of 82.2(2)° (**5**) and 87.1(1)° (**10**). As a result, the *o*-methyl groups are efficiently shielding the vacant boron p-orbitals from above and below, which explains the chemical inertness of the B−C bonds. All key metrical parameters of the $DBA(Mes)_2$ fragments in **5** and **10** are essentially the same as in parent **2**[18] and therefore do not merit further discussion. In 2,6-Br_2-$DBA(Mes)_2$ (**5**), the charge density at Br(1) is 14% less than expected for one bromo substituent; the missing charge density is located close to H(5). Thus, **5** either cocrystallizes together with a small fraction of 2,7-Br_2-$DBA(Mes)_2$ (**6**) and/or **5** is disordered over two positions about a 2-fold axis running through the boron atoms. The second explanation is supported by the fact that a similar phenomenon has been observed in the crystal structure analysis of the isomerically pure compound 2,6-dibromo-9,10-dimesitylanthracene (cf., the Supporting Information for more details).

Derivatization of Halogenated 9,10-Dimesityl-9,10-dihydro-9,10-diboraanthracenes through Stille Coupling. Attempts at a metal/bromine exchange on **5**/**6** with elemental Mg or *n*-BuLi in THF were not met with success. An initial color change from yellow to deep red did not persist, and the final color of the reaction mixtures was a dark brown. When Me_3SiCl was added as an electrophilic quencher at various points in time, complex mixtures containing the respective starting material, free mesitylene, and numerous unidentified other species were obtained. We assume that electron injection into the Br−C σ^* orbital competes with the reduction of the low-lying DBA-centered π^* orbital at the first stages of the reactions. In line with this view, parent **2** is easily reducible with elemental Li to the red-colored dilithium salt $Li_2[\mathbf{2}]$.[17,25]

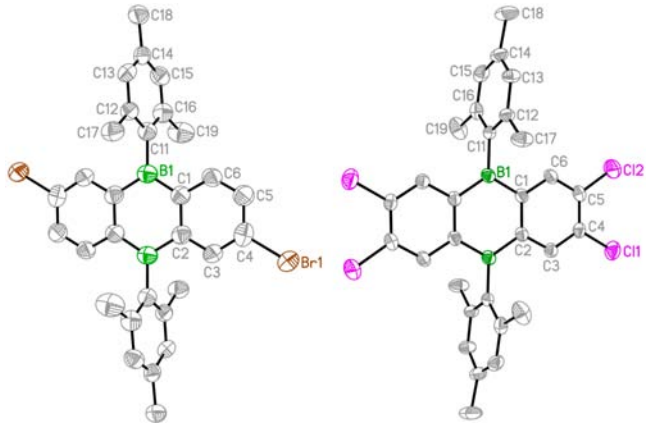

Figure 3. Molecular structure of **5** (left) and **10** (right) in the solid state. Displacement ellipsoids are drawn at the 50% probability level; H atoms have been omitted for clarity. The bromine atoms in **5** are disordered over two positions with an occupancy ratio of 0.858(3):0.142(3); only the major orientation is shown. Selected bond lengths (Å), bond angles (deg), and dihedral angle (deg): **5**, B(1)−C(1) 1.550(9), B(1)−C(2A) 1.572(10), B(1)−C(11) 1.576(9), C(1)−C(2) 1.435(8), C(4)−Br(1) 1.878(7); C(1)−B(1)−C(2A) 118.7(5), C(1)−B(1)−C(11) 120.9(6), C(2A)−B(1)−C(11) 120.4(6); Ar(B(1))//Ar(C(11)) 82.2(2). **10**, B(1)−C(1) 1.571(5), B(1)−C(2A) 1.558(5), B(1)−C(11) 1.571(5), C(1)−C(2) 1.417(5), C(4)−Cl(1) 1.716(3), C(5)−Cl(2) 1.712(3); C(1)−B(1)−C(2A) 118.6(3), C(1)−B(1)−C(11) 119.4(3), C(2A)−B(1)−C(11) 121.9(3); Ar(B(1))//Ar(C(11)) 87.1(1). Symmetry transformation used to generate equivalent atoms: **5**, A, $-x + 3/2$, $-y + 1/2$, $-z + 3/2$; **10**, A, $-x + 1$, $-y + 1$, $-z + 2$.

We identified the best-suited Pd-catalyzed C−C-coupling strategy for the further modification of **5**−**13** by screening three different methods to introduce phenyl rings into the molecular scaffolds. Suzuki-type protocols led to extensive decomposition, because under the basic conditions required to cleave the $(HO)_2B$−Ph bond, B−C bonds within the $DBA(Mes)_2$ frameworks are obviously activated as well.[40] Negishi-type protocols failed to give any transformation, while the Stille-coupling reaction was immediately successful.

5/**6** and **10** were converted in toluene with $PhSnBu_3$ into **20**/**21** and **22** using 2.5 mol % $[Pd(PtBu_3)_2]$ per halogen atom as the catalyst (Scheme 4). The reactions can be conducted with comparable results either in a closed glass vessel with Young valve (120 °C, 1 d) or in a microwave synthesizer (170 °C, 45 min). The fully substituted target compounds were easily separated from partially substituted and protodehalogenated side products by column chromatography (silica gel, hexane/$CHCl_3$) and isolated in 40% yield each.

The quantitative Br/Ph exchange in **20**/**21** and **22** is unequivocally evident from the ^1H and $^{13}C\{^1H\}$ NMR spectra of the compounds. Not only does the number of resonances correspond to the proposed symmetry of the molecules, but an inspection of the proton integral ratios confirms the presence of 2 and 4 phenyl rings in **20**/**21** and **22**, respectively. The molecular structure of the centrosymmetric isomer 2,6-Ph_2-$DBA(Mes)_2$ (**20**) was further corroborated by X-ray crystallography (cf., the Supporting Information for full details). In contrast to 2,6-Br_2-$DBA(Mes)_2$ (**5**), **20** is not disordered in the

dx.doi.org/10.1021/ja406766e | J. Am. Chem. Soc. 2013, 135, 12892−12907

Scheme 4. Stille-Type Pd-Catalyzed C−C-Coupling Reactions of 5/6 or 10 with $PhSnBu_3$[a]

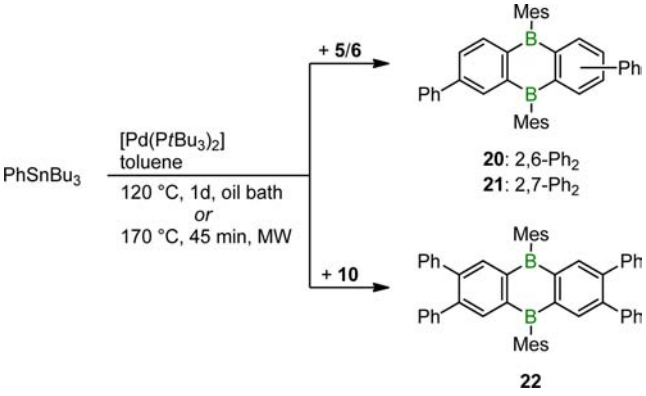

[a]MW = microwave irradiation.

crystal lattice; the dihedral angle between one phenyl ring and the DBA core amounts to 33.9(1)°.

As alluded to above, the DBA(Mes)$_2$ moiety possesses an energetically low-lying LUMO, essentially identical to the π^* orbital of the DBA core.[25] We therefore reasoned that pronounced effects on the optoelectronic properties of the DBA(Mes)$_2$ fragment will arise if it is equipped with electron-donating substituents such as 2-thienyl and *p*-*N*,*N*-diphenylaminophenyl.[41] Starting from corresponding halogenated symmetrical or unsymmetrical DBA(Mes)$_2$ derivatives shown in Scheme 2 and $ThSnBu_3$ or $Ph_2NphSnBu_3$, we have prepared compounds **23**−**31** (Th = 2-thienyl, ph = *p*-phenylene; Figure 4) through the Stille-type protocol outlined in Scheme 4. The complete series of possible substitution patterns, which will provide an opportunity to study detailed structure−property relationships, was realized for the 2-thienyl derivatives. Isolated yields were generally excellent, even with the tetrachlorinated starting material **10**. The solubilities of the compounds **23**−**28** in common organic solvents are considerably improved as compared to those of the starting materials, while the air and moisture stabilities remain the same. Importantly, 2,6-(2-thienyl)$_2$-DBA(Mes)$_2$ (**23**) could be separated from the 2,7-isomer **24** via HPLC. All compounds **23**−**28** are yellow-colored, some of them with a greenish tint. Solutions show turquoise to green emission already when they are exposed to daylight; strong solid-state fluorescence is observed upon irradiation with a UV lamp (366 nm).

The introduction of *p*-*N*,*N*-diphenylaminophenyl substituents was facile for the dibrominated starting materials (i.e., **5**/**6**→**29**/**30**), whereas the yields reproducibly dropped to 45% in the case of **31** (cf., 81% obtained for **26**). Contrary to the 2-thienyl species **23**/**24** and **26**, **29**/**30** and **31** decompose in nondried, nondegassed solvents within several hours (NMR spectroscopic and UV/vis spectroscopic control). This instability, together with the fact that **29** and **30** showed virtually identical retention times on the HPLC column, precluded the isomer separation. The orange- (**29**/**30**) to red-colored (**31**) compounds exhibit strong orange to red fluorescence in solution as well as in the solid state (see below).

The identity of compounds **23**−**31** was confirmed by NMR spectroscopy, and **23**, **26**−**28**, and **31** were further characterized by X-ray crystallography (Figure 5; cf., the Supporting Information for **27** and **31**). Each of the centrosymmetric compounds **23** and **26** crystallizes with two crystallographically

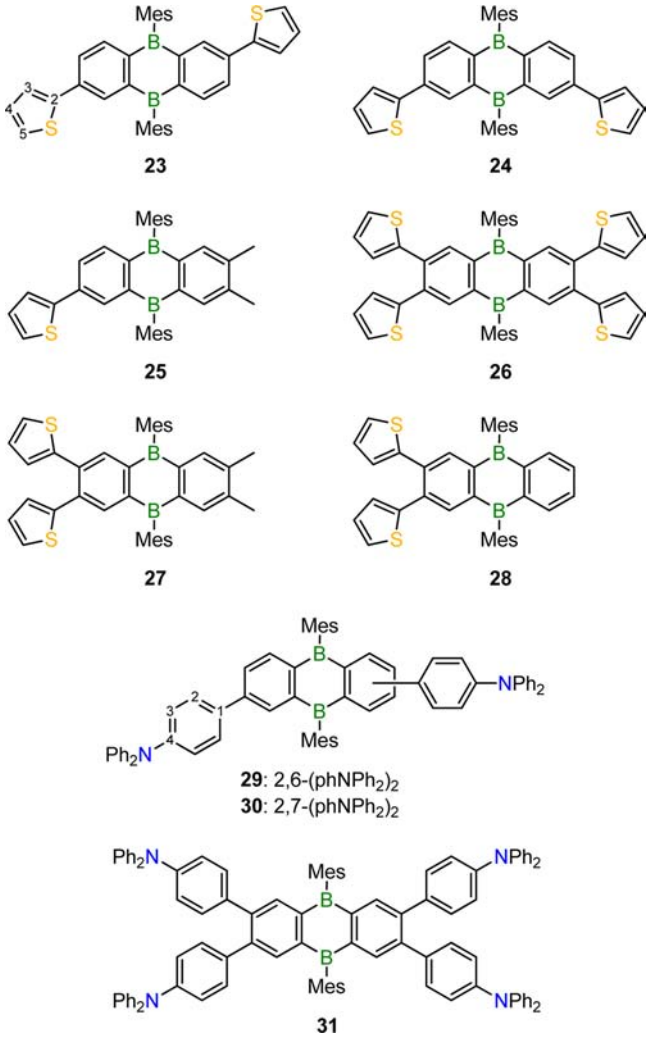

Figure 4. The complete series of accessible substitution patterns as exemplified for 2-thienyl-functionalized DBAs (**23**−**28**) as well as the *p*-*N*,*N*-diphenylaminophenyl derivatives **29**/**30** and **31** were synthesized according to the protocol outlined in Scheme 4 (ph = *p*-phenylene).

independent molecules in the asymmetric unit (**23**$_A$, **23**$_B$; **26**$_A$, **26**$_B$). In **23**$_A$ and **23**$_B$, the dihedral angles between the 2-thienyl rings and the DBA planes amount to 28.1(2)° and 30.5(2)°, respectively. The two vicinal 2-thienyl substituents in **28** define one small (30.4(1)°) and one large (68.5(3)°) dihedral angle with the DBA core; two markedly different interplanar angles are also found in the cases of **26**$_A$ (42.1(2)°, 55.9(2)°) and **26**$_B$ (37.8(2)°, 67.0(2)°). We take these structural peculiarities as an indication that each *o*-phenylene ring tends to maintain maximum π-conjugation with one 2-thienyl donor, even if this requires sacrificing the donor capacity of a second substituent.

All-Carbon Analogues of 2,6-Substituted DBA(Mes)$_2$ Derivatives. Detailed studies, in which the optoelectronic properties of a specific organo-heteroelement system have been thoroughly characterized and compared to those of an isostructural all-carbon congener, are lacking. For example, neutral, closed-shell structural analogues of boroles, borepins, or the highly popular dimesitylboryl group simply do not exist. The situation is different in the case of DBA derivatives, which are isostructural to anthracenes and isoelectronic to the elusive anthracene dications.

dx.doi.org/10.1021/ja406766e | J. Am. Chem. Soc. 2013, 135, 12892−12907

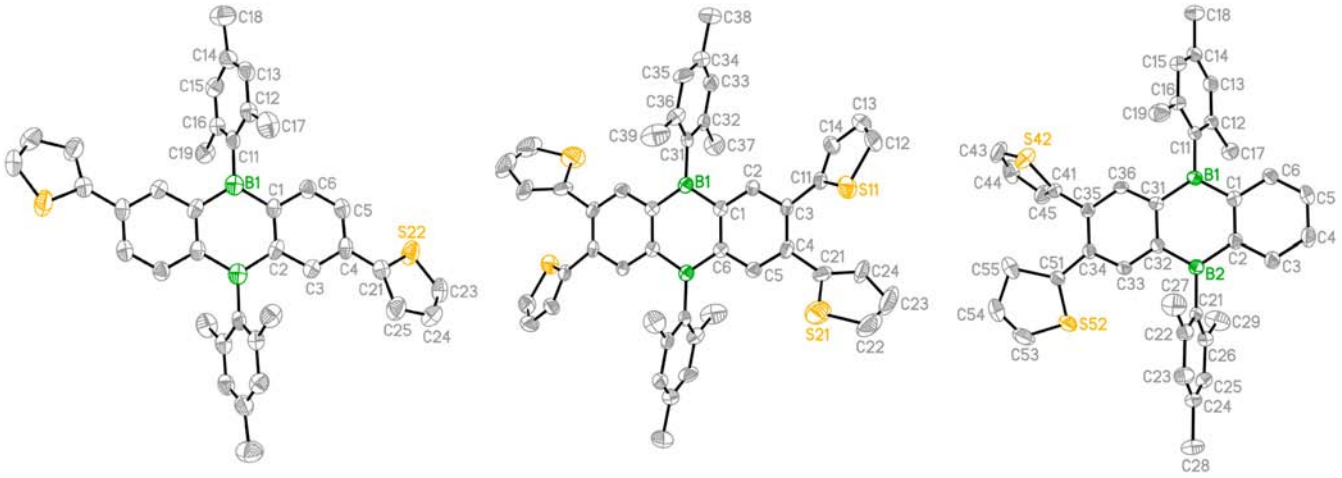

Figure 5. Molecular structure of $\mathbf{23}_A$ (left), $\mathbf{26}_A$ (middle), and **28** (right) in the solid state. Displacement ellipsoids are drawn at the 50% probability level; H atoms have been omitted for clarity. The thiophene moieties in $\mathbf{23}_A$ are disordered with respect to a 180° rotation about the C(4)−C(21) bond causing S(22) and C(25) to exchange positions; the occupancy ratio is 0.727(8):0.273(8); only the major orientation is shown. The 2-thienyl moieties in **28** are disordered with respect to a 180° rotation about the C(34)−C(51) bond [the C(35)−C(41) bond] causing S(52) and C(55) [S(42) and C(45)] to exchange positions; the occupancy ratio is 0.538(4):0.462(4) [0.750(4):0.250(4)]; only the major orientation is shown. Selected bond lengths (Å), bond angles (deg), and dihedral angles (deg): $\mathbf{23}_A$, B(1)−C(1) 1.559(9), B(1)−C(2A) 1.578(8), B(1)−C(11) 1.566(9), C(1)−C(2) 1.414(8); C(1)−B(1)−C(2A) 117.6(5), C(1)−B(1)−C(11) 120.8(5), C(2)−B(1)−C(11) 121.6(5); Ar(B(1))//Ar(C(11)) 76.5(2), Ar(C(4))//Ar(C(21)) 28.1(2). $\mathbf{26}_A$, B(1)−C(1) 1.576(6), B(1)−C(6A) 1.559(7), B(1)−C(31) 1.569(7), C(1)−C(6) 1.413(6), C(11)−S(11) 1.722(5), C(12)−S(11) 1.709(6), C(21)−S(21) 1.708(7), C(22)−S(21), 1.688(9); C(1)−B(1)−C(6A) 117.8(4), C(1)−B(1)−C(31) 118.5(4), C(6A)−B(1)−C(31) 123.7(4), C(11)−S(11)−C(12) 91.6(3), C(21)−S(21)−C(22) 92.4(4); Ar(B(1))//Ar(C(31)) 85.7(2), Ar(C(3))//Ar(C(11)) 42.1(2), Ar(C(4))//Ar(C(21)) 55.9(2). **28**, B(1)−C(1) 1.562(3), B(1)−C(31) 1.565(3), B(1)−C(11) 1.571(3), B(2)−C(2) 1.556(3), B(2)−C(32) 1.560(3), B(2)−C(21) 1.569(3), C(1)−C(2) 1.413(3), C(31)−C(32) 1.417(3); C(1)−B(1)−C(31) 118.68(18), C(1)−B(1)−C(11) 120.58(18), C(31)−B(1)−C(11) 120.73(18), C(2)−B(2)−C(32) 118.69(18), C(2)−B(2)−C(21) 121.67(19), C(32)−B(2)−C(21) 119.64(18), C(35)−C(34)−C(51) 124.96(19), C(34)−C(35)−C(41) 122.75(18); Ar(B(1))//Ar(C(11)) 76.7(1), Ar(B(2))//Ar(C(21)) 88.7(1), Ar-(C(34))//Ar(C(51)) 30.4(1), Ar(C(35))//Ar(C(41)) 68.5(1). Symmetry transformation used to generate equivalent atoms: $\mathbf{23}_A$, A, $-x + 2$, $-y + 1$, $-z + 1$; $\mathbf{26}_A$, A, $-x + 1$, $-y + 1$, $-z + 1$.

The all-carbon relatives **32**−**36** of the $DBA(Mes)_2$ derivatives **2**, **5**, **20**, **23**, and **29** were prepared with the aim to compare the π charge-density distributions, the crystal packing motifs, and the optoelectronic properties of both classes of compounds.[42] Pristine **32** is literature-known;[25] 2,6-dibromo-9,10-dimesitylanthracene (**33**) was synthesized in a one-pot procedure by treating 2,6-dibromoanthraquinone[43] first with MesMgBr and then with $SnCl_2/HCl_{aq}$ (Scheme 5). Subsequent Suzuki- or Stille-type coupling reactions afforded the corresponding phenyl (**34**), 2-thienyl (**35**), and *p*-*N*,*N*-diphenylaminophenyl (**36**) derivatives (Scheme 5).

$^{13}C\{^1H\}$ NMR spectroscopy is a useful tool to map the π charge-density distributions in arenes, because the shielding of a specific arene carbon atom depends linearly on the π-electron density at this position, and its chemical shift remains largely unaffected by ring current anisotropies.[44] The DBA derivatives **5**, **20**, **23**, and **29** are isoelectronic to $[\mathbf{33}]^{2+}$−$[\mathbf{36}]^{2+}$ and therefore show the predictable deshielding of their C-1 to C-4 carbon nuclei (e.g., the C-1 nuclei are deshielded by 13.3−14.0 ppm). In contrast, the ^{13}C resonance patterns of analogous DBA and anthracene derivatives are essentially superimposable. NMR spectroscopy thus provides no evidence for a stronger π donation of the electron-rich substituents to the DBA moieties than to the anthracene cores.

The proton chemical shift differences between the *p*- and *o*-CH_3 groups in mesityl-substituted cyclic conjugated π systems provide a measure of the magnetic anisotropy and thereby of the degree of aromaticity in these systems.[45] For the four boron species, these $\Delta\delta$ values range between 0.27 and 0.31 ppm, whereas the $\Delta\delta$ values of the all-carbon compounds **33**−**36** are found in the interval 0.63−0.72 ppm ($\Delta\delta = \delta(p\text{-}CH_3) - \delta(o\text{-}CH_3)$). It is thus obvious that the ring currents in the central anthracene C_6 rings are significantly larger than those in the formally antiaromatic central B_2C_4 rings. The $\Delta\delta$ values of our $DBA(Mes)_2$ derivatives compare well with those of other mesityl-substituted antiaromatic boron heterocycles, that is, 6,13-dimesityl-6,13-dihydro-6,13-diborapentacene (0.37 ppm),[29] *B*-mesityldibenzoborole (0.17 ppm),[46] and *B*-mesityltetraphenylborole (0.27 ppm);[47] in stark contrast, $\Delta\delta$ equals

Scheme 5. Synthesis Route to the All-Carbon Analogues 33−36[a]

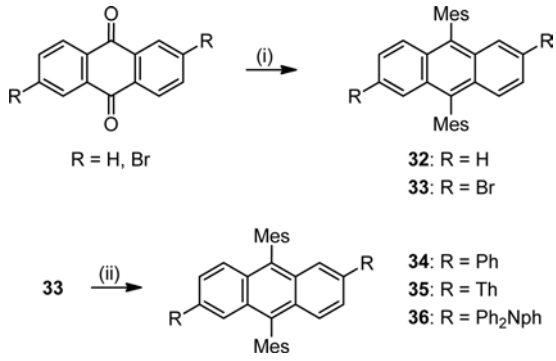

[a]Th = 2-thienyl, ph = *p*-phenylene. (i) (1) +MesMgBr (3 equiv in THF), 60 °C, 2 h; (2) +$SnCl_2 \cdot 2H_2O$ (2 equiv) in 5 M HCl_{aq}. (ii) **34**: +$PhB(OH)_2$ (2.4 equiv), $[Pd(PtBu_3)_2]$ (6 mol %), Na_2CO_3 (5.3 equiv), toluene/H_2O/EtOH (3:2:1), microwave synthesizer 170 °C, 45 min. **35**, **36**: +$RSnBu_3$ (2.4 equiv), $[Pd(PtBu_3)_2]$ (6 mol %), toluene, oil bath 120 °C, 1 d or microwave synthesizer 170 °C, 45 min.

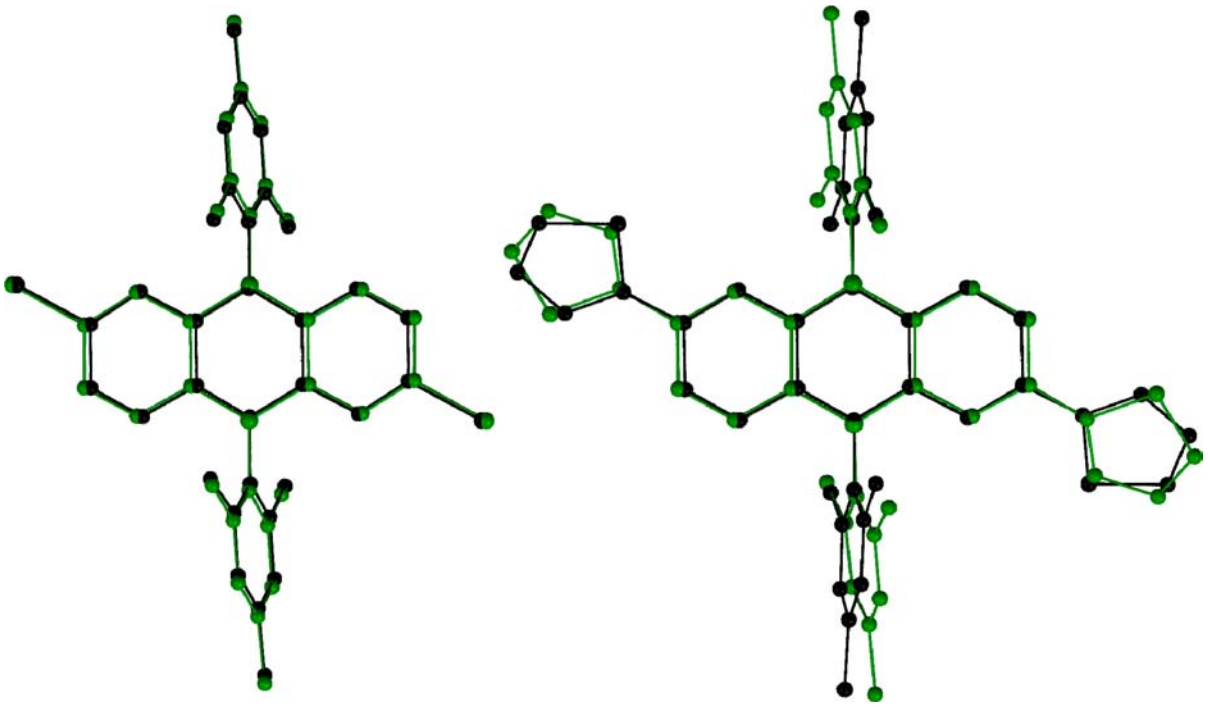

Figure 6. Overlays of the DBA derivatives (green) with their all-carbon congeners (black) **5**/**33** (left) and **23**$_A$/**35** (right).

0.91 ppm for the formally aromatic *B*-mesityldibenzoborepin,[48] similar to the anthracenes **33**–**36**.

Compounds **33** and **35** were also characterized by X-ray crystallography. The bromo-substituted **33** is isostructural with its DBA congener **5**; a least-squares fit of the tricyclic cores yields an rms deviation of 0.123 Å (cf., Figure 6 for an overlay of both molecular structures). The structural similarities are going so far that the bromine atoms in **33** even exhibit the same kind of disorder as discussed above in the case of **5**. The only noteworthy differences in the geometrical parameters of **5** and **33** relate to the B–C bonds, which are longer than the corresponding C–C bonds in **33**. Moreover, we note no significant deviation between the lengths of the B–C_{exo} single bond (1.576(9) Å) and the average B–C_{endo} bond (1.561 Å). On the contrary, an appreciably shorter average C–C_{endo} bond (1.407 Å) as compared to the C–C_{exo} bond (1.498(7) Å) is found in **33** (Δ = 0.091 Å). This feature reflects a low degree of B═C_{endo} π bonding in the DBA(Mes)$_2$ derivative as opposed to significant C═C_{endo} double-bond character in its anthracene analogue and nicely matches the differences in the ring-current effects assessed above by NMR spectroscopy.

Even though the crystal structures of the 2-thienyl species **23** and **35** are not comparable because **35** crystallizes together with 1 equiv of toluene, their molecular structures are as much alike as those of the bromo-substituted pair (cf., the dihedral angle 2-thienyl//DBA = 28° (**35**), 28° (**23**$_A$), 30° (**23**$_B$); Figure 6 shows an overlay of **35** and **23**$_A$). With respect to the B═C_{endo}/C═C_{endo} double-bond character, we come to the same conclusion as outlined above (cf., the Supporting Information for more details).

Optoelectronic Properties. The DBA derivatives **5**/**6**, **10**, and **23**–**31** as well as the all-carbon analogues **33**, **35**, and **36** were investigated by cyclic voltammetry. For a discussion of the electrochemical data (cf., Table 1, Figure 7), it is helpful to first consider the cyclic voltammograms of the parent species 9,10-dimesityl-9,10-dihydro-9,10-diboraanthracene (**2**) and

Table 1. Electrochemical Data[a]

	$E_{1/2}$ in [V] vs FcH/FcH$^+$
5/**6**	−1.59[c]
10	−1.38[c]
23/**24**	−1.71, −2.48[d]
25	−1.83, −2.63[d]
26	−1.59, −2.39[d]
27	−1.79, −2.84[e]
28	−1.62, −2.41,[d] −3.16[e]
29/**30**[b]	+0.38;[f] +0.10;[f] −2.11[c]
31	+0.60;[f] +0.30;[f] −1.86[c]
33	−2.20,[e] −2.33,[e] −2.61,[e] −3.15,[e] −3.39[e]
35	−2.37, −3.00,[e] −3.42[e]
36	+0.55, −2.46,[d] −2.96, −3.4[e]

[a]Dried and degassed THF; supporting electrolyte, [nBu$_4$N][PF$_6$] (0.1 mol L^{-1}); scan rate, 200 mV s^{-1}. [b]$E_{1/2}$ calibrated against internal FcH*/FcH*$^+$ and recalculated versus FcH/FcH$^+$ ($E_{1/2}$(FcH*/FcH*$^+$) = −0.45 V vs FcH/FcH$^+$; FcH* = (C$_5$Me$_5$)$_2$Fe). [c]Decomposition occurs at potential values more cathodic than approximately −2.5 V. [d]Quasi-reversible redox wave. [e]E_{pc} value. [f]E_{pa} value.

9,10-dimesitylanthracene (**32**).[25] The potential value of $E_{1/2}$ = −1.84 V required for the DBA-centered one-electron reduction of **2** is more anodic by 0.75 V than that necessary for the monoreduction of **32** ($E_{1/2}$ = −2.59 V). Both processes are reversible. In contrast, the second one-electron reduction is fully reversible only for **2** ($E_{1/2}$ = −2.73 V), but shows features of chemical irreversibility in the case of **32** (E_{pc} = −3.40 V).

The DBA species compiled in Table 1 reveal a behavior similar to that of compound **2**, with the following modifications: (i) Halogenation of the DBA scaffold (i.e., **5**/**6**, **10**) somewhat facilitates the injection of a first electron. At potential values more cathodic than approximately −2.5 V, however, the compounds undergo extensive decomposition. We currently assume that reductive cleavage of the C–Cl/Br bonds competes with the incorporation of a second electron

dx.doi.org/10.1021/ja406766e | J. Am. Chem. Soc. 2013, 135, 12892–12907

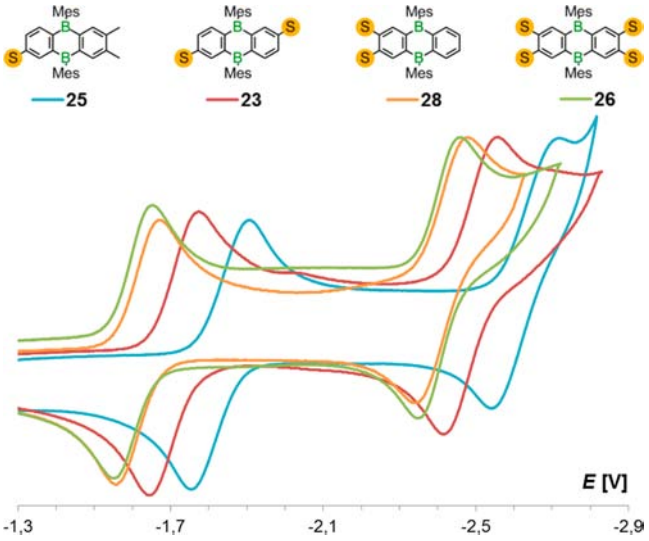

Figure 7. Normalized cyclic voltammograms of **23**, **25**, **26**, and **28** as solutions in THF at room temperature; supporting electrolyte, $[n\mathrm{Bu_4N}][\mathrm{PF_6}]$ (0.1 mol $\mathrm{L^{-1}}$); scan rate, 200 mV $\mathrm{s^{-1}}$; vs $\mathrm{FcH/FcH^+}$. In the case of **28**, an additional irreversible redox process takes place at E_{pc} = −3.16 V.

into the DBA π-electron system (cf., the above discussion of attempted Grignard or lithium−halogen exchange reactions on **5**/**6** and **10**). (ii) With an increasing number of 2-thienyl substituents, the corresponding DBA derivatives become more easily reducible (cf., Figure 7). (iii) An introduction of *p*-*N*,*N*-diphenylaminophenyl substituents leads to the occurrence of two more redox events in the positive potential regime, likely involving the electron-rich peripheral groups. In summary, similar to pristine **2**, most of the substituted 9,10-dimesityl-9,10-dihydro-9,10-diboraanthracenes are electrochemically well-behaved and significantly better electron acceptors than the all-carbon congeners.

Unless noted otherwise, the UV/vis absorption and fluorescence spectra discussed in the following paragraphs were recorded in $\mathrm{C_6H_6}$.[49] We first turn our attention to the UV/vis spectral properties of the DBAs and to a comparison with the organic model systems **32**−**36** (Table 2). The longest-wavelength absorptions of the all-carbon compounds **32**−**36** show the characteristic vibrational fine structure typical of anthracene derivatives. As compared to **32**, any substitutions at the phenylene rings led to slight bathochromic shifts. Moreover, a number of intense hypsochromic bands occur (Table 2), which are yet irrelevant for the color of the molecules or the calculation of Stokes shifts/band gaps and therefore do not merit further discussions.

Most importantly, no indications for (intramolecular) charge-transfer transitions are apparent in the UV/vis spectra of **33**−**36**.

This situation changes upon going to the DBA species for which the longest-wavelength absorptions generally exhibit tails extending far into the low-energy regime (e.g., **10**, λ_{max} = 354 nm, onset at 450 nm; **22**, λ_{max} = 370 nm, onset at 440 nm; **26**, λ_{max} = 388 nm, onset at 485 nm). The red-orange compounds **29**/**30** and **31**, which bear strongly electron-donating *p*-*N*,*N*-diphenylaminophenyl groups at the electron-poor DBA center, are characterized by independent, broad charge-transfer bands at λ_{max} = 458 nm (ε = 11 600 $\mathrm{mol^{-1}\ dm^3\ cm^{-1}}$; onset at 530 nm) and 459 nm (ε = 34 000 $\mathrm{mol^{-1}\ dm^3\ cm^{-1}}$; onset at 540 nm), respectively.

The fluorescence spectra of the two classes of compounds show striking differences already for the two parent molecules **32** and **2**. 9,10-Dimesitylanthracene (**32**) fluoresces at λ_{em} = 403 nm with a high quantum yield of 80%; the position of the emission band is essentially independent of solvent polarity. $\mathrm{DBA(Mes)_2}$ (**2**), in contrast, hardly fluoresces at all (λ_{em} = 460 nm; ϕ_f = 3%), and the emission wavelength shows pronounced positive solvatochromism ($\mathrm{C_6H_{12}}$, λ_{em} = 415 nm; $\mathrm{CH_2Cl_2}$, λ_{em} = 489 nm; Δ = 3650 $\mathrm{cm^{-1}}$). Anthracene fluorescence is known to originate from $\pi\rightarrow\pi^*$ transitions,[50] whereas the emission of **2** has been attributed to twisted intramolecular charge transfer (TICT) transitions between the orthogonal DBA and mesityl units.[21,25]

Dibromination of **32** results in considerably reduced quantum yields due to the fluorescence quenching effect of heavy-atoms[50] (cf., **33**; ϕ_f = 53%). Because the boron-containing molecule **2** already is a very poor emitter, halogenation in this case has no significant further attenuating effect on the quantum yields of the compounds obtained (**5**/**6**, **10**).

The introduction of two strong *p*-*N*,*N*-diphenylaminophenyl electron donors into the parent systems (**32**, **2**) shifts the emission bands of the all-carbon (**36**) as well as the boron-containing species (**29**/**30**) by approximately 4000 $\mathrm{cm^{-1}}$ to the bathochromic side (Table 2). A decisive difference between the two classes of compounds is, however, apparent for the trend in the quantum yields. The quantum yield of **32** is very high (ϕ_f = 80%) and does not change much for **36** (ϕ_f = 72%). Yet, in the case of the boron-doped species, we have literally switched on a bright fluorescence upon going from **2** (ϕ_f = 3%) to **29**/**30** (ϕ_f = 69%) by generating a distinct donor−acceptor−donor triad.

The availability of **23**−**28** offers a means to investigate in detail how the optical properties of the $\mathrm{DBA(Mes)_2}$ fluorophore change when the number or the positional arrangement of its moderately electron-donating 2-thienyl substituents is varied (Table 2; Figure 8). We first note a continuous red-shift of the emission wavelengths with an increasing number of 2-thienyl groups, which covers an overall range of 2800 $\mathrm{cm^{-1}}$ (**25** (λ_{em} = 469 nm) → **23**/**27**/**28** (λ_{em} = 486/515/524 nm) → **26** (λ_{em} = 540 nm)). Second, the fluorescence maxima of the 2,6- and the 2,3-isomer **23** and **28** differ by as much as 1320 $\mathrm{cm^{-1}}$. Changing the positional arrangement of the pendant groups is thus a similarly powerful set screw to modify the optoelectronic properties of DBA fluorophores as is the introduction of an additional 2-thienyl moiety (cf., **25** → **27**: Δ = 1900 $\mathrm{cm^{-1}}$).

For an optimization of quantum yields, the proper position of the 2-thienyl rings turns out to be an even more decisive factor than a large absolute number of substituents. For example, the quantum efficiency of **23** (ϕ_f = 44%) can be improved to ϕ_f = 70% (**28**) by moving the two 2-thienyl groups onto the same phenylene fragment. On the other hand, ϕ_f decreases considerably upon proceeding from disubstituted **23** or **28** to the tetrasubstituted derivative **26** (ϕ_f = 25%). As a general trend, best quantum efficiencies seem to be achievable by gathering all 2-thienyl substituents at the same side of the molecule (cf., **25**, **27**, and **28**). Consequently, donor−acceptor dyads are apparently more efficient emitters than donor−acceptor−donor triads (cf., **23**, **26**).

Finally, Figure 9 compiles the UV/vis fluorescence spectra of selected $\mathrm{DBA(Mes)_2}$ species and of their all-carbon congeners.

While the anthracene derivatives emit in the near-ultraviolet to blue region of the visible light spectrum, the DBA derivatives

Table 2. Photophysical Data

	in C_6H_6								for thin films		
	λ_{abs} [nm] (ε [mol^{-1} dm^3 cm^{-1}])	λ_{onset} [nm]	E_G^{opt} [eV][a]	λ_{ex} [nm]	λ_{em} [nm]	ϕ_f [%][b]	Stokes shift [cm^{-1}][c]	E_{HOMO}/E_{LUMO} [eV][d]	λ_{abs} [nm]	λ_{em} [nm][e]	ϕ_f [%][b]
5/6	352 (9900)	440	2.8	350	500	<1	8400	−6.0/−3.2	358[f]	520[f]	<1[f]
									395[f,g]		
									424[f,g]		
10	354 (10 000)	450	2.7	350	504	<1	8400	−6.1/−3.4	350[f]	488[f]	<1[f]
									411[f,g]		
20/21	368 (15 200)	430	2.9	365	446	6	4800	−/−	370	462	6
					460				408[g]		
22	304 (110 000)	440	2.8	305	481	11	6200	−/−	306[f]	489[f]	22[f]
	370 (21 700)								370[f]		
									410[f,g]		
23	307 (43 700)	470	2.6	305	486	44	4800	−/−	306	485[h]	8
	340 (41 800)				broad				338	506[h]	
	396 (20 800)								395	522[h]	
23/24	306 (66 300)	470	2.6	305	490	45	4800	−5.7/−3.1	306	499	9
	340 (47 500)				broad				336		
	396 (25 700)								392		
25	319 (23 400)	450	2.7	315	469[h]	66	3300	−5.7/−3.0	316	486	22
	366 (7900)				494[h]				367	broad	
	406 (5700)								405		
26	332 (66 500)	485	2.6	355	540	25	7300	−5.8/−3.2	325	538	12
	388 (26 000)								388		
									450[g]		
27	316 (42 300)	460	2.7	315	515	72	7500	−5.8/−3.1	316	529	9
	372 (14 100)								371		
									430[g]		
28	316 (41 400)	460	2.7	315	524	70	7900	−5.9/−3.2	318	522	19
	370 (12 800)								372		
									423[g]		
29/30	336 (40 300)	530	2.3	450	563	69	4100	−5.0/−2.7	338	574	10
	458 (11 600)		(2.2)[i]					(−4.9/−2.7)[i]	464		
31	308 (110 000)	540	2.3	460	594	60	5000	−5.2/−2.9	308	599	22
	340 (119 000)		(2.2)[i]					(−5.1/−2.9)[i]	337		
	459 (34 000)								505[g]		
33	350 (2000)[h]	420	3.0	365	414[h]	53	420	−5.6/−2.6	350[h]	444[h]	4
	366 (3900)[h]				437[h]				367[h]	470[h]	
	386 (5600)[h]				462[h]				387[h]	499[h]	
	407 (5600)[h]				495[h]				409[h]		
34	301 (48 000)	430	2.9	300	429[h]	72	560	−/−	304	436[h]	4
	375 (2900)[h]				455[h]				377[h]	460[h]	
	396 (4500)[h]				484[h]				396[h]	487[h]	
	419 (4100)[h]								419[h]		
35	315 (74 100)	455	2.7	328	452[h]	37	760	−5.1/−2.4	319[g]	483[h]	1
	328 (102 000)				479[h]				331	517[h]	
	389 (9000)[h]								393[h]		
	409 (14 300)[h]								412[h]		
	437 (13 900)[h]								438[h]		
36	305 (25 000)	465	2.7	360	478[h]	72	2000	−5.1/−2.4	310[f]	493[f]	1.5[f]
	360 (32 000)		(3.0)[i]		498[h]			(−5.4/−2.4)[i]	360[f]		
	418 (8000)[h]								420[f]		
	437 (8000)[h]								443[f,g]		

[a]Band gap values were calculated from the onset wavelengths (λ_{onset}) of the absorption spectra. [b]Quantum yields were determined by a calibrated integrating sphere. [c]The Stokes shifts given represent the difference between the longest absorption and shortest emission wavelengths. [d]Energy levels were calculated from CV data (E_{LUMO} = −4.8 eV − $E_{1/2}^{red}$; FcH/FcH$^+$ = −4.8 eV vs vacuum level) and from the optically determined band gap ($E_{HOMO} = E_{LUMO} - E_G^{opt}$). [e]$\lambda_{ex}$ = 315 nm. [f]Poor film homogeneity. [g]Shoulder. [h]Vibronic fine structure. [i]Value calculated exclusively from CV data.

cover the blue to orange wavelengths. In this respect, the two classes of compounds are therefore not competitors, but nicely complement each other. Most band gaps fall in the intervals between 2.6 and 2.9 eV for the DBA species and 2.7−3.0 eV for their all-carbon analogues (Table 2); significantly smaller band gaps are only found for the *p*-aminophenyl-DBAs **29**/**30**

dx.doi.org/10.1021/ja406766e | J. Am. Chem. Soc. 2013, 135, 12892−12907

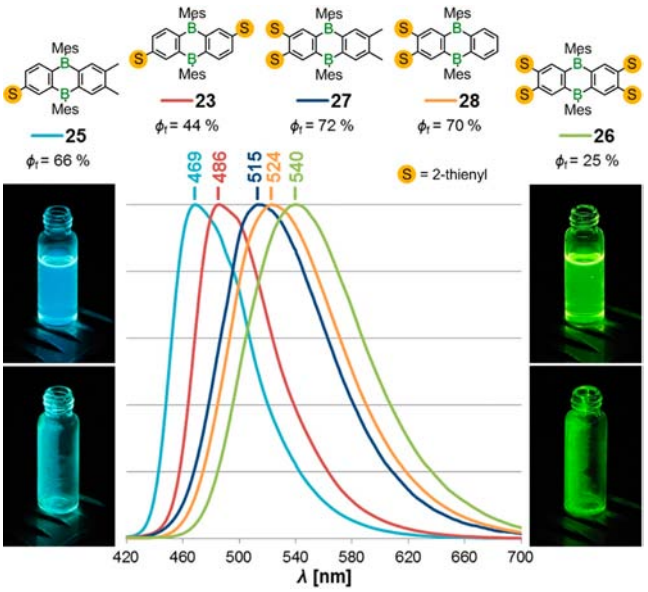

Figure 8. Normalized emission spectra of the thienylated DBA derivatives **23** and **25**–**28** in C_6H_6 and photographs (hand-held UV-lamp with λ_{ex} = 366 nm) of the fluorescence of **25** (left) and **26** (right) both in C_6H_6 (top) and in the solid state (bottom).

(2.3 eV) and **31** (2.3 eV).[50] Differences between the acceptor strengths of a central DBA versus a 9,10-anthrylene moiety are apparent from much more pronounced solvatochromic effects in the fluorescence spectra of the DBA derivatives (cf., the Supporting Information for more details). Comparing DBA dyads with DBA triads, the still limited data set does not allow for a clear-cut statement as to whether the former or the latter show stronger solvatochromism.

Despite their strong fluorescence in dilute solutions,[51,52] many anthracene derivatives tend to show a poor performance in the solid state, mainly due to π stacking, excimer formation, and self-quenching phenomena.[53] Even though we expected that the bulky orthogonal mesityl substituents in **32**–**36** should help to avoid unwanted π stacking, thin films of these compounds never gave ϕ_f values larger than 4%.[54] The weak solid-state fluorescence is thus likely attributable to self-quenching resulting from the small Stokes shifts of **32**–**36**. In line with that, the corresponding DBA derivatives **20**/**21**, **23**, and **29**/**30**, which possess larger Stokes shifts (Table 2; for a direct comparison of **23** and **35**, cf., Figure 10), give quantum yields of 6%, 8%, and 10%, respectively. The best solid-state quantum efficiencies are observed for the tetraphenylated DBA **22**, the monothienyl DBA **25** (Figure 8, bottom left), and the tetrakis(*p*-aminophenyl) DBA **31** with ϕ_f = 22% for each of them.

CONCLUSION

4-Bromo-1,2-bis(trimethylsilyl)benzene (**3**) and 4,5-dichloro-1,2-bis(trimethylsilyl)benzene (**4**) are excellent starting materials for the synthesis of the C-halogenated, B-mesitylated 9,10-dihydro-9,10-diboraanthracene (DBA) derivatives 2,6/2,7-Br_2-DBA(Mes)$_2$ (**5**/**6**) and 2,3,6,7-Cl_4-DBA(Mes)$_2$ (**10**). We have thoroughly studied the course of the reaction between **3** and BBr_3 by in situ NMR spectroscopy and identified 4-bromo-1,2-bis(dibromoboryl)benzene (**16**) as the key intermediate of the DBA assembly; we also identified an intramolecular Br/Me-exchange reaction in the intermediate 4-bromo-1-dibromoboryl-2-trimethylsilylbenzene (**14**) as the major yield-limiting process. The transient diborylbenzene **16** can be trapped by electron-rich aromatics (e.g., *o*-xylene) in preparatively useful yields, which provides a convenient access route to unsymmetrically

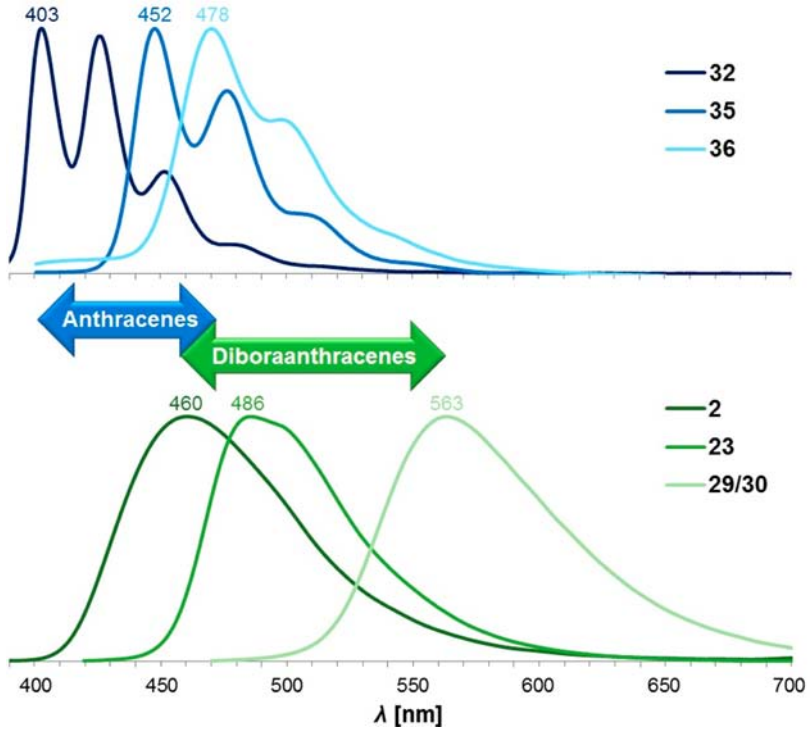

Figure 9. Normalized emission spectra of the anthracene derivatives **32**,[25] **35**, and **36** (top) and the corresponding DBA derivatives **2**,[25] **23**, and **29**/**30** (bottom) in C_6H_6.

dx.doi.org/10.1021/ja406766e | J. Am. Chem. Soc. 2013, 135, 12892–12907

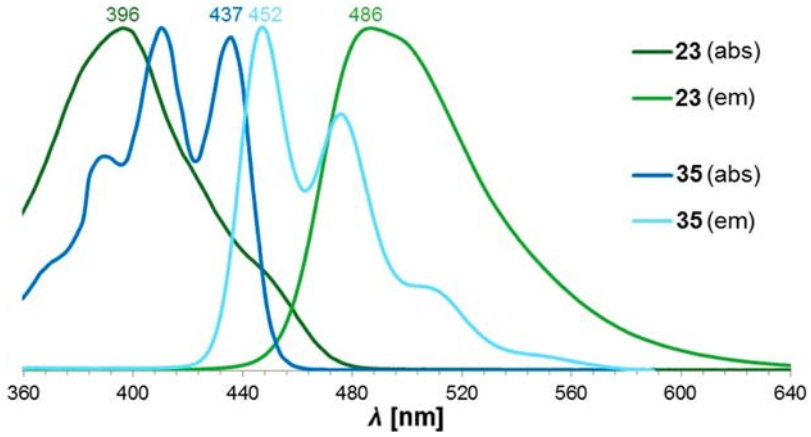

Figure 10. Normalized UV/vis absorption (dark green, **23**; dark blue, **35**) and emission spectra (light green, **23**; light blue, **35**) in C_6H_6. The Stokes shifts differ strongly for the two congeners with values of 94 nm (4800 cm^{-1}) for **23** and 15 nm (760 cm^{-1}) for **35**.

brominated DBAs (the same applies to the dichlorinated analogue).

Stille-type coupling protocols allow the further functionalization of chlorinated as well as brominated DBA(Mes)$_2$ derivatives. Using 2-thienyl as a model substituent, we have prepared a number of benchtop stable mono- (**25**), di- (**23**, **24**, **27**, **28**), and tetrasubstituted (**26**) DBA(Mes)$_2$ species and found that already a variation of the number and/or the positional distribution of the donor groups enables a tuning of the emission wavelength from 469 nm (blue) to 540 nm (green). The corresponding quantum yields range between 25% and 72%. There is no clear-cut correlation between the number of appended 2-thienyl groups and the quantum efficiency observed; however, donor−acceptor dyads tend to be better emitters than donor−acceptor−donor triads. Stronger donors than the 2-thienyl ring exert an even stronger effect on the photoluminescence properties; that is, the 2,3,6,7-tetrakis-(*p*-aminophenyl)-DBA(Mes)$_2$ **31** fluoresces at approximately 600 nm (red).

The molecular design achieved for our C-substituted DBA(Mes)$_2$ species results in air and water stabilities that are similar to those of classical organic compounds commonly used in organic electronics. Thus, we can now gain the full benefits of boron doping, which become evident upon direct comparison with the isostructural anthracene analogues: (i) The first electron affinities of our DBAs are on average higher by as much as 0.6 eV. (ii) The full tunable interval of emission colors falls in the visible range of the spectrum (blue to orange), while anthracenes emit in the near-ultraviolet to blue wavelength regime. (iii) Our DBAs show significant solid-state quantum yields, whereas those of the corresponding anthracenes are negligible.

EXPERIMENTAL SECTION

General Considerations. Unless otherwise specified, all reactions were carried out under dry nitrogen using Schlenk techniques. Hexane, toluene, *o*-xylene, THF, and C_6D_6 were dried over Na/benzophenone and distilled prior to use. The compounds 4-bromo-1,2-bis-(trimethylsilyl)benzene **3**,[32] 4,5-dichloro-1,2-bis(trimethylsilyl)-benzene **4**,[31] and tri-*n*-butyl(*p*-*N*,*N*-diphenylaminophenyl)stannane[55] were synthesized according to literature procedures. The microwave-assisted reactions were performed using a Biotage Initiator$^+$ microwave synthesizer with vials obtained from Biotage.

NMR spectra were recorded on Bruker DPX 250, Avance 300, and Avance 400 spectrometers. Chemical shifts are referenced to (residual) solvent signals (^{1}H/^{13}C{^{1}H}: $CDCl_3$, 7.26/77.16 ppm; C_6D_6, 7.15/128.06 ppm; C_6D_{12}, 1.38/26.43 ppm), external $BF_3{\cdot}Et_2O$ (^{11}B{^{1}H}: 0.00 ppm), or external $SiMe_4$ (^{29}Si INEPT: 0.00 ppm). Abbreviations: s = singlet, d = doublet, dd = doublet of doublets, t = triplet, vt = virtual triplet, m = multiplet, n.o. = signal not observed, Ph = phenyl, ph = *p*-phenylene, Th = 2-thienyl. Signals of boron-bonded carbon atoms were typically broadened beyond detection in the ^{13}C{^{1}H} NMR spectra; their chemical shift values were determined using the cross peaks in the HMBC spectra. UV/vis absorption and emission spectra were recorded on a Varian Cary 50 Scan UV/vis spectrophotometer and a Jasco FP-8300 spectrofluorometer, respectively. The absolute fluorescence quantum yields (ϕ_f) were determined using a calibrated integrating sphere system (ILF-835 100 mm diameter Integrating Sphere; Jasco), a quantum yield calculation program (FWQE-880; Jasco), and highly diluted samples of at least five different optical densities in each measurement. For the determination of the quantum yields of thin films, at least four films of varying thicknesses were generated for each compound by evaporation of differently concentrated samples in $CHCl_3$ at 100 °C on a quartz-glass surface. Electrochemical measurements were performed at room temperature by using an EG&G Princeton Applied Research 263A potentiostat with a platinum disk working electrode (diameter 2.00 mm). The reference electrode was a silver wire on which AgCl had been deposited by immersing the wire into HCl/HNO_3 (3:1). The solvent (THF) was dried at room temperature over sodium without added benzoquinone and degassed by five freeze−pump−thaw cycles. [nBu$_4$N][PF$_6$] (0.1 mol/L) was employed as the supporting electrolyte. All potential values are referenced against the FcH/FcH$^+$ couple ($E_{1/2}$ = 0 V). Combustion analyses were performed by the Microanalytical Laboratory of the University of Frankfurt or by the Microanalytical Laboratory Pascher (Remagen, Germany).

General Procedure for the Preparation of the Halogenated DBA(Mes)$_2$ Derivatives 5−13. A thick-walled glass ampule was charged with the respective 1,2-bis(trimethylsilyl)benzene **3** or **4** (3.6 mmol), BBr_3 (1.0 mL, 2.6 g, 11 mmol), and the appropriate solvent or solvent mixture (5 mL). The ampule was flame-sealed under vacuum and subsequently heated to 120 °C for 1.5 d. The dark yellow-colored solution obtained was cooled to room temperature, transferred to a Schlenk flask, and evaporated to dryness at 100 °C in vacuo. The resulting solid was dissolved in toluene (10 mL) without further purification, and a THF solution of MesMgBr (0.86 M, 8.4 mL, 7.2 mmol) was added dropwise with stirring over 10 min at 0 °C. The reaction mixture was allowed to warm to room temperature overnight, quenched with aqueous saturated NH_4Cl (10 mL), and the organic phase was separated with a separation funnel. The aqueous phase was extracted with $CHCl_3$ (3 × 10 mL), and all organic phases were combined, washed with H_2O (2 × 10 mL), dried over anhydrous $MgSO_4$, and filtered. All volatiles were removed from the filtrate in vacuo, and the residual crude material was purified by column chromatography. The products obtained are air- and water-stable

dx.doi.org/10.1021/ja406766e | J. Am. Chem. Soc. 2013, 135, 12892−12907

yellow powders, which show almost no fluorescence in solution or the solid state. The synthesis has been scaled up to 10 mmol of 1,2-bis(trimethylsilyl)benzene without losses in isolated yields.

Synthesis of 2,6/2,7-Br_2-DBA(Mes)$_2$ (5/6). The synthesis was performed according to the general procedure for the preparation of halogenated DBA(Mes)$_2$ derivatives. For a maximum yield, hexane was used as the solvent in the first reaction step. The purification of the crude product by column chromatography (silica gel, hexane:$CHCl_3$ = 3:1) afforded a mixture of the two isomers **5** and **6** in a 1:1 ratio as a yellow powder (the isomer distribution was determined by ^{1}H NMR spectroscopy). Overall yield: 0.44 g (0.77 mmol, 43%). To achieve maximum selectivity for the 2,6-isomer (**5**:**6** = 3:2), the reaction was conducted in C_6H_6; workup was the same as described above. Overall yield: 0.32 g (0.56 mmol, 31%). **5** crystallized upon slow evaporation of a $CHCl_3$ solution of **5**/**6** in the form of light brown plates that were suitable for X-ray crystal structure analysis. Attempts to separate the two isomers by HPLC using either reversed-phase Reprosil-Pur C18-AQ or normal phase Nucleosil columns (10 μm, 250 × 20 mm) with various eluents were not successful. Analytical data for mixtures of **5**/**6**, NMR data of **5**, ^{1}H NMR (300.0 MHz, $CDCl_3$): δ 2.04 (s, 12H; *o*-CH_3), 2.40 (s, 6H; *p*-CH_3), 6.94 (s, 4H; MesH), 7.46 (d, $^3J_{HH}$ = 7.8 Hz, 2H; H-4,8), 7.61 (dd, $^3J_{HH}$ = 7.8 Hz, $^4J_{HH}$ = 2.1 Hz, 2H; H-3,7), 7.70 (d, $^4J_{HH}$ = 2.1 Hz, 2H; H-1,5). ^{11}B NMR (96.3 MHz, $CDCl_3$): δ 71 ($h_{1/2}$ = 900 Hz). ^{13}C NMR (75.4 MHz, $CDCl_3$): δ 21.5 (*p*-CH_3), 22.8 (*o*-CH_3), 127.4 (MesC-3,5), 130.4 (C-2,6), 136.8 (C-3,7), 137.6 (MesC-4), 138.0 (MesC-2,6), 139.2 (MesC-1), 140.9 (C-4,8), 141.5 (C-1,5), 142.8, 146.9 (CB). NMR data of **6** (only the resonances mentioned could be unequivocally identified; missing resonances are overlapping with signals of the 2,6-isomer), ^{1}H NMR (300.0 MHz, $CDCl_3$): δ 2.03, 2.05 (2 × s, 2 × 6H; *o*-CH_3), 2.39, 2.41 (2 × s, 2 × 3H; *p*-CH_3), 7.47 (d, $^3J_{HH}$ = 7.8 Hz, 2H; H-4,5), 7.69 (d, $^4J_{HH}$ = 2.1 Hz, 2H; H-1,8). ^{13}C NMR (75.4 MHz, $CDCl_3$): δ 21.5, 21.5 (*p*-CH_3), 22.8, 22.9 (*o*-CH_3), 127.4, 127.5 (MesC-3,5), 130.2 (C-2,7), 136.9 (C-3,6), 137.5, 137.7 (MesC-4), 137.9, 138.1 (MesC-2,6), 140.7 (C-4,5), 141.6 (C-1,8), 142.9, 146.9 (CB). Anal. Calcd for $C_{30}H_{28}B_2Br_2$ (569.96): C, 63.22; H, 4.95. Found: C, 62.60; H, 5.15.

Synthesis of 2-Br-6,7-Me_2-DBA(Mes)$_2$ (9). The synthesis was performed according to the general procedure for the preparation of halogenated DBA(Mes)$_2$ derivatives. A 1:1 mixture of hexane/*o*-xylene was used as the solvent in the first reaction step. The purification of the crude product by column chromatography (silica gel, hexane:$CHCl_3$ = 3:1) afforded a mixture of **5**/**6** and **9** in a 3:2:10 ratio as a yellow powder (the product distribution was determined by ^{1}H NMR spectroscopy). Overall yield **5**/**6** and **9**: 0.32 g (33%) containing 0.21 g (22% yield) of **9**. NMR data of **9**, ^{1}H NMR (300.0 MHz, $CDCl_3$): δ 2.06, 2.07 (2 × s, 2 × 6H; *o*-CH_3), 2.23 (s, 6H; DBA-CH_3), 2.41, 2.42 (2 × s, 2 × 3H; *p*-CH_3), 6.94 (s, 4H; MesH), 7.39 (d, $^3J_{HH}$ = 7.8 Hz, 1H; H-4), 7.39, 7.40 (2 × s, 2 × 1H; H-5, H-8), 7.55 (dd, $^3J_{HH}$ = 7.8 Hz, $^4J_{HH}$ = 2.1 Hz, 1H; H-3), 7.63 (d, $^4J_{HH}$ = 2.1 Hz, 1H; H-1). ^{11}B NMR (96.3 MHz, $CDCl_3$): δ 69 ($h_{1/2}$ = 800 Hz). ^{13}C NMR (75.4 MHz, $CDCl_3$): δ 20.2 (DBA-CH_3), 21.4, 21.5 (*p*-CH_3), 22.7, 22.8 (*o*-CH_3), 127.1, 127.2 (MesC-3,5), 129.5 (C-2), 136.1 (C-3), 136.9, 137.0 (MesC-4), 138.0, 138.1 (MesC-2,6), 140.2 (MesC-1), 140.8, 140.8, 140.9, 141.0 (C-1,4,5,8), 143.1, 143.3 (C-6,7), 147.5 (CB).

Synthesis of Cl_4-DBA(Mes)$_2$ (10). The synthesis was performed according to the general procedure for the preparation of halogenated DBA(Mes)$_2$ derivatives. Hexane was used as the solvent in the first reaction step. Cl_4DBA(Br)$_2$ crystallized already in the ampule in the form of thick colorless needles, which were several centimeters long and suitable for X-ray crystal structure analysis. The purification of crude **10** by column chromatography (silica gel, hexane:$CHCl_3$ = 3:1) afforded the product as a microcrystalline yellow solid. Overall yield: 0.59 g (1.1 mmol, 60%). **10** crystallized upon slow evaporation of its $CHCl_3$/pentane solution in the form of yellow blocks that were suitable for X-ray crystal structure analysis. ^{1}H NMR (300.0 MHz, $CDCl_3$): δ 2.03 (s, 12H; *o*-CH_3), 2.41 (s, 6H; *p*-CH_3), 6.95 (s, 4H; MesH), 7.64 (s, 4H; H-1,4,5,8). ^{11}B NMR (96.3 MHz, $CDCl_3$): δ 74 ($h_{1/2}$ = 1000 Hz). ^{13}C NMR (75.4 MHz, $CDCl_3$): δ 21.4 (*p*-CH_3), 22.8 (*o*-CH_3), 127.6 (MesC-3,5), 137.8 (MesC-2,6), 138.0 (MesC-4), 138.9 (C-2,3,6,7), 140.2 (MesC-1), 140.7 (C-1,4,5,8), 144.3 (CB). Anal. Calcd for $C_{30}H_{26}B_2Cl_4$ (549.93): C, 65.52; H, 4.77. Found: C, 65.03; H, 4.60.

Synthesis of 2,3-Cl_2-6,7-Me_2-DBA(Mes)$_2$ (13). The synthesis was performed according to the general procedure for the preparation of halogenated DBA(Mes)$_2$ derivatives. A 1:1 mixture of hexane/*o*-xylene was used in the first reaction step. The purification of the crude product by column chromatography (silica gel, hexane:$CHCl_3$ = 3:1) afforded a mixture of **10** and **13** in a 1:7 ratio as a yellow powder (the product distribution was determined by ^{1}H NMR spectroscopy; it varies between individual experiments, and the average distribution of four runs is given). Overall yield: 0.32 g (34%) containing 0.27 g (30% yield) of **13**. NMR data of **13**, ^{1}H NMR (300.0 MHz, $CDCl_3$): δ 2.08 (s, 12H; *o*-CH_3), 2.25 (s, 6H; DBA-CH_3), 2.43 (s, 6H; *p*-CH_3), 6.96 (s, 4H; MesH), 7.42 (s, 2H; H-5,8), 7.59 (s, 2H; H-1,4). ^{11}B NMR (96.3 MHz, $CDCl_3$): δ 69 ($h_{1/2}$ = 1300 Hz). ^{13}C NMR (75.4 MHz, $CDCl_3$): δ 20.2 (DBA-CH_3), 21.4 (*p*-CH_3), 22.8 (*o*-CH_3), 127.3 (MesC-3,5), 137.2 (MesC-4), 137.9 (C-2,3), 138.0 (Mes-C2,6), 140.0 (C-1,4), 140.1 (MesC-1), 141.1 (C-5,8), 142.6 (CB), 143.4 (C-6,7), 145.1 (CB).

General Procedure for the Stille-type Coupling Reactions. The respective halogenated DBA(Mes)$_2$ derivative or derivative mixture (100 μmol DBA equiv), [Pd(P*t*Bu$_3$)$_2$] (2.5 mol % per halogen atom), and the appropriate tri-*n*-butylstannane (1.2 equiv per halogen atom) in toluene (3 mL) were heated with stirring either in an oil bath (120 °C, 1 d) or in a microwave synthesizer (170 °C, 45 min). The reaction mixture was allowed to cool to room temperature, all volatiles were removed in vacuo, and the residual crude material was purified by column chromatography. Because all target products are highly fluorescent even when adsorbed on the column, the product bands can easily be identified on the stationary phase with the help of a hand-held UV-lamp (λ_{ex} = 366 nm). The synthesis has been scaled up to 0.5 mmol of halogenated DBA equiv without losses in isolated yields.

Synthesis of Ph_4-DBA(Mes)$_2$ (22). The synthesis was performed according to the general procedure for the Stille-type coupling reactions using **10** (100 μmol). The purification of the crude product by column chromatography (silica gel, hexane:$CHCl_3$ = 5:1) afforded **22** as an air- and water-stable yellow powder showing a turquoise fluorescence both in the solid state and in solution. Yield: 29 mg (40 μmol, 40%). ^{1}H NMR (300.0 MHz, $CDCl_3$): δ 2.18 (s, 12H; *o*-CH_3), 2.33 (s, 6H; *p*-CH_3), 6.87 (s, 4H; MesH), 7.05−7.08 (m, 8H; PhH-2,6), 7.16−7.19 (m, 12H; PhH-3,4,5), 7.70 (s, 4H; H-1,4,5,8). ^{11}B NMR (96.3 MHz, $CDCl_3$): δ 73 ($h_{1/2}$ = 1500 Hz). ^{13}C NMR (75.4 MHz, $CDCl_3$): δ 21.4 (*p*-CH_3), 23.1 (*o*-CH_3), 126.9 (PhC-4), 127.2 (MesC-3,5), 128.0 (PhC-3,5), 130.0 (PhC-2,6), 136.7 (MesC-4), 137.9 (MesC-2,6), 140.5 (MesC-1), 141.2 (C-1,4,5,8), 141.2 (PhC-1), 144.9 (CB), 145.2 (C-2,3,6,7). Anal. Calcd for $C_{54}H_{46}B_2$ (716.57): C, 90.51; H, 6.47. Found: C, 90.20; H, 6.67.

Synthesis of 2,6/2,7-(2-Thienyl)$_2$-DBA(Mes)$_2$ (23/24). The synthesis was performed according to the general procedure for the Stille-type coupling reactions using **5** (60 μmol) and **6** (40 μmol). The purification of the crude product by column chromatography (silica gel, hexane:$CHCl_3$ = 3:1) afforded **23**/**24** (3:2 ratio) as an air-and water-stable yellow-green powder showing a turquoise fluorescence both in the solid state and in solution. Yield of **23**/**24**: 46 mg (80 μmol, 80%). **23** can be separated from **24** by HPLC using a normal-phase Nucleosil semipreparative column (10 μm, 250 × 20 mm) and hexane as the eluent; the fraction containing **24** was, however, still contaminated with **23**. **23** crystallized in the form of yellow X-ray quality needles upon layering a $CHCl_3$ solution of **23**/**24** with pentane. Analytical data of **23**, ^{1}H NMR (300.0 MHz, $CDCl_3$): δ 2.10 (s, 12H; *o*-CH_3), 2.42 (s, 6H; *p*-CH_3), 6.94 (s, 4H; MesH), 7.05 (dd, $^3J_{HH}$ = 4.9 Hz, 3.8 Hz, 2H; ThH-4), 7.26−7.29 (m, 4H; ThH-3, ThH-5), 7.65 (m, 4H; H-3,7, H-4,8), 7.85 (m, 2H; H-1,5). ^{11}B NMR (96.3 MHz, $CDCl_3$): δ 70 ($h_{1/2}$ = 1000 Hz). ^{13}C NMR (75.4 MHz, $CDCl_3$): δ 21.5 (*p*-CH_3), 22.9 (*o*-CH_3), 124.6, 126.2 (ThC-3, ThC-5), 127.2 (MesC-3,5), 128.3 (ThC-4), 130.1 (C-3,7 or C-4,8), 136.0 (C-1,5), 137.0 (MesC-4), 138.1 (MesC-2,6), 139.1 (C-2,6), 139.9 (C-3,7 or C-4,8), 140.6 (MesC-1), 144.0 (ThC-2), 146.3 (CB). The following analytical data were obtained on mixtures of **23**/**24**. NMR data of **24**

(only the resonances mentioned could be unequivocally identified; missing resonances are overlapping with signals of the 2,6-isomer), ^{13}C NMR (75.4 MHz, $CDCl_3$): δ 21.4, 21.5 (*p*-CH_3), 22.8, 22.9 (*o*-CH_3), 124.5, 126.2 (ThC-3, ThC-5), 127.1, 127.3 (MesC-3,5), 128.4 (ThC-4), 130.3 (C-3,6 or C-4,5), 136.2 (C-1,8), 137.0 (MesC-4), 137.9, 138.2 (MesC-2,6), 138.9 (C-2,7 or ThC-2), 139.6 (C-3,6 or C-4,5). Anal. Calcd for $C_{38}H_{34}B_2S_2$ (576.39): C, 79.18; H, 5.95; S, 11.13. Found: C, 78.27*; H, 6.16; S, 10.84. "*" represents incomplete combustion due to boron carbide formation.

Synthesis of 2-(2-Thienyl)-6,7-Me$_2$-DBA(Mes)$_2$ (25). The synthesis was performed according to the general procedure for the Stille-type coupling reactions using a mixture of **5**/**6** (33 μmol) and **9** (67 μmol). **23**/**24** and **25** can be separated from each other by column chromatography (silica gel, hexane:$CHCl_3$ = 5:1) and thereby obtained as analytically pure samples. The target product **25** is an air- and water-stable yellow-green powder showing a turquoise fluorescence both in the solid state and in solution. Yield: 32 mg (61 μmol, 91%). ^{1}H NMR (300.0 MHz, $CDCl_3$): δ 2.09 (s, 12H; *o*-CH_3), 2.24 (s, 6H; DBA-CH_3), 2.42 (s, 6H; *p*-CH_3), 6.94, 6.94 (2 × s, 2 × 2H; MesH), 7.03 (dd, $^3J_{HH}$ = 5.0, 3.7 Hz, 1H; ThH-4), 7.24−7.28 (m, 2H; ThH-3, ThH-5), 7.41, 7.42 (2 × s, 2 × 1H; H-5, H-8), 7.55 (d, $^3J_{HH}$ = 7.6 Hz, 1H; H-4), 7.62 (dd, $^3J_{HH}$ = 7.6 Hz, $^4J_{HH}$ = 1.8 Hz, 1H; H-3), 7.78 (d, $^4J_{HH}$ = 1.8 Hz, 1H; H-1). ^{11}B NMR (96.3 MHz, $CDCl_3$): δ 69 ($h_{1/2}$ = 1000 Hz). ^{13}C NMR (75.4 MHz, $CDCl_3$): δ 20.2, 20.2 (DBA-CH_3), 21.5, 21.5 (*p*-CH_3), 22.8, 22.9 (*o*-CH_3), 124.4, 126.0 (ThC-3, ThC-5), 127.0, 127.1 (MesC-3,5), 128.3 (ThC-4), 130.0 (C-3), 135.7 (C-1), 136.7 (MesC-4), 138.0, 138.2 (MesC-2,6), 138.7 (C-2), 139.3 (C-4), 140.7, 140.9 (C-5, C-8), 140.9 (MesC-1), 142.7, 142.9 (C-6, C-7), 144.2 (ThC-2), 146.1 (CB). Anal. Calcd for $C_{38}H_{34}B_2S$ (576.43): C, 82.78; H, 6.95; S, 6.14. Found: C, 82.58; H, 6.87; S, 6.31.

Synthesis of (2-Thienyl)$_4$-DBA(Mes)$_2$ (26). The synthesis was performed according to the general procedure for the Stille-type coupling reactions using **10** (100 μmol). The purification of the crude product by column chromatography (silica gel, hexane:$CHCl_3$ = 3:1) afforded **26** as an air- and water-stable yellow powder showing a yellow-green fluorescence in the solid state. The compound is completely air- and water-stable also in solution and fluoresces with a pronounced positive solvatochromism (cyclohexane, green; C_6H_6 and $CHCl_3$, yellow-green; THF, yellow; acetone, yellow-orange). Yield: 60 mg (81 mmol, 81%). **26** crystallized in the form of yellow X-ray quality needles upon layering its $CHCl_3$ solution with pentane. ^{1}H NMR (300.0 MHz, $CDCl_3$): δ 2.15 (s, 12H; *o*-CH_3), 2.37 (s, 6H; *p*-CH_3), 6.88 (dd, $^3J_{HH}$ = 3.6 Hz, $^4J_{HH}$ = 1.1 Hz, 4H; ThH-3 or ThH-5), 6.90 (s, 4H; MesH), 6.94 (dd, $^3J_{HH}$ = 5.0, 3.6 Hz, 4H; ThH-4), 7.26 (dd, $^3J_{HH}$ = 5.0 Hz, $^4J_{HH}$ = 1.1 Hz, 4H; ThH-3 or ThH-5), 7.76 (s, 4H; H-1,4,5,8). ^{11}B NMR (96.3 MHz, $CDCl_3$): δ 70 ($h_{1/2}$ = 1500 Hz). ^{13}C NMR (75.4 MHz, $CDCl_3$): δ 21.4 (*p*-CH_3), 23.1 (*o*-CH_3), 126.9 (ThC-3 or ThC-5), 127.1 (ThC-4), 127.3 (MesC-3,5), 127.8 (ThC-3 or ThC-5), 137.0 (MesC-4), 138.0 (MesC-2,6), 138.4 (C-2,3,6,7), 140.0 (MesC-1), 141.5 (C-1,4,5,8), 142.3 (ThC-2), 144.7 (CB). Anal. Calcd for $C_{46}H_{38}B_2S_4$ (740.62): C, 74.59; H, 5.17; S, 17.32. Found: C, 73.59*; H, 5.25; S, 17.17. "*" represents incomplete combustion due to boron carbide formation.

Synthesis of 2,3-(2-Thienyl)$_2$-6,7-Me$_2$-DBA(Mes)$_2$ (27). The synthesis was performed according to the general procedure for the Stille-type coupling reactions using a mixture of **10** (13 μmol) and **13** (87 μmol). **26** and **27** can be separated from each other by column chromatography (silica gel, hexane:$CHCl_3$ = 4:1) and thereby obtained as analytically pure samples. The target product **27** is an air- and water-stable green powder showing a yellow-green fluorescence in the solid state and in solution. Yield: 50 mg (83 μmol, 95%). **27** crystallized upon slow evaporation of its $CHCl_3$/hexane solution in the form of yellow needles that were suitable for X-ray crystal structure analysis. ^{1}H NMR (300.0 MHz, $CDCl_3$): δ 2.10 (s, 12H; *o*-CH_3), 2.24 (s, 6H; DBA-CH_3), 2.39 (s, 6H; *p*-CH_3), 6.84 (dd, $^3J_{HH}$ = 3.6 Hz, $^4J_{HH}$ = 1.2 Hz, 2H; ThH-3 or ThH-5), 6.91−6.93 (m, 6H; MesH, ThH-4), 7.24 (dd, $^3J_{HH}$ = 5.1, $^4J_{HH}$ = 1.2 Hz, 2H; ThH-3 or ThH-5), 7.40 (s, 2H; H-5,8), 7.67 (s, 2H; H-1,4). ^{11}B NMR (96.3 MHz, $CDCl_3$): δ 70 ($h_{1/2}$ = 900 Hz). ^{13}C NMR (75.4 MHz, $CDCl_3$): δ 20.2 (DBA-CH_3), 21.4 (*p*-CH_3), 23.0 (*o*-CH_3), 126.7 (ThC-3 or ThC-5), 127.1 (ThC-4), 127.1 (MesC-3,5), 127.7 (ThC-3 or ThC-5), 136.7 (MesC-4), 138.0 (C-2,3), 138.1 (MesC-2,6), 140.7 (MesC-1), 140.8 (C-5,8), 141.0 (C-1,4), 142.5 (ThC-2), 142.9 (C-6,7), 144.7 (CB). Anal. Calcd for $C_{40}H_{38}B_2S_2$ (604.48): C, 79.48; H, 6.34; S, 10.61. Found: C, 79.08; H, 6.35; S, 10.55.

Synthesis of 2,6/2,7-(*p*-*N*,*N*-Diphenylaminophenyl)$_2$-DBA-(Mes)$_2$ (29/30). The synthesis was performed according to the general procedure for the Stille-type coupling reactions using **5** (60 μmol) and **6** (40 μmol). The purification of the crude product by column chromatography (silica gel, hexane:$CHCl_3$ = 3:1) afforded **29**/**30** (3:2 ratio) as an air- and water-stable orange powder showing an orange fluorescence in the solid state. In solution, the compound fluoresces with a pronounced positive solvatochromism (cyclohexane, green; C_6H_6 and $CHCl_3$, orange; THF, red). In nondried, non-degassed solvents, the compound decomposes over the course of 1 d. Attempts to separate the two isomers by HPLC using either reversed-phase Reprosil-Pur C18-AQ or normal phase Nucleosil columns (10 μm, 250 × 20 mm) with various eluents were not successful. Yield: 70 mg (78 μmol, 78%). Analytical data for mixtures of **29**/**30**, NMR data of **29**, ^{1}H NMR (300.0 MHz, $CDCl_3$): δ 2.12 (s, 12H; *o*-CH_3), 2.40 (s, 6H; *p*-CH_3), 6.93 (s, 4H; MesH), 7.01−7.08 (m, 8H; PhH-4, phH-3,5), 7.10−7.13 (m, 8H; PhH-2,6), 7.24−7.29 (m, 8H; PhH-3,5), 7.37−7.39 (m, 4H; phH-2,6), 7.61−7.68 (m, 4H; H-3,7, H-4,8), 7.82−7.83 (m, 2H; H-1,5). ^{11}B NMR (96.3 MHz, $CDCl_3$): n.o. ^{13}C NMR (75.4 MHz, $CDCl_3$): δ 21.5 (*p*-CH_3), 22.9 (*o*-CH_3), 123.3, 123.4 (phC-3,5, PhC-4), 124.9 (PhC-2,6), 127.1 (MesC-3,5), 128.1 (phC-2,6), 129.5 (PhC-3,5), 131.0 (C-3,7), 134.2 (phC-1), 136.8 (MesC-4), 137.0 (C-1,5), 138.1 (MesC-2,6), 139.7 (C-4,8), 141.1 (MesC-1), 143.7 (CB), 145.4 (C-2,6), 147.6 (PhC-1), 148.0 (phC-4). NMR data of **30** (only the resonances mentioned could be unequivocally identified; missing resonances are overlapping with signals of the 2,6-isomer), ^{1}H NMR (300.0 MHz, $CDCl_3$): δ 2.37, 2.42 (2 × s, 2 × 3H; *p*-CH_3), 6.90, 6.96 (2 × s, 2 × 2H; MesH). ^{13}C NMR (75.4 MHz, $CDCl_3$): δ 21.3 (*p*-CH_3), 22.8, 23.0 (*o*-CH_3), 127.1 (MesC-3,5), 137.9, 138.3 (Mes-C2,6). Anal. Calcd for $C_{66}H_{56}B_2N_2$ (898.79): C, 88.20; H, 6.28; N, 3.12. Found: C, 87.47; H, 6.41; N, 3.55.

Synthesis of (*p*-*N*,*N*-Diphenylaminophenyl)$_4$-DBA(Mes)$_2$ (31). The synthesis was performed according to the general procedure for the Stille-type coupling reactions using **10** (100 μmol). The purification of the crude product by column chromatography (silica gel, hexane:$CHCl_3$ = 3:1) afforded **31** as an air- and water-stable red powder showing an orange-red fluorescence in the solid state. In solution, the compound fluoresces intensely with a pronounced positive solvatochromism (cyclohexane, green; C_6H_6, orange; $CHCl_3$, light red; THF, red; acetone, dark red). In nondried, nondegassed solutions, **31** decomposes over the course of 1 d. Yield: 63 mg (45 μmol, 45%). **31** crystallized in the form of thin red X-ray quality needles upon layering its $CHCl_3$ solution with hexane. ^{1}H NMR (300.0 MHz, $CDCl_3$): δ 2.19 (s, 12H; *o*-CH_3), 2.37 (s, 6H; *p*-CH_3), 6.88−6.94 (m, 20H; phH, MesH), 6.99−7.02 (m, 8H; PhH-4), 7.07−7.09 (m, 16H; PhH-2,6), 7.21−7.25 (m, 16H; PhH-3,5), 7.66 (s, 4H; H-1,4,5,8). ^{11}B NMR (96.3 MHz, $CDCl_3$): n.o. ^{13}C NMR (75.4 MHz, $CDCl_3$): δ 21.4 (*p*-CH_3), 23.2 (*o*-CH_3), 122.6 (phC-3,5), 123.1 (PhC-4), 124.7 (PhC-2,6), 127.2 (MesC-3,5), 129.4 (PhC-3,5), 130.8 (phC-2,6), 135.1 (phC-1), 136.6 (MesC-4), 138.2 (MesC-2,6), 140.8 (C-1,4,5,8), 141.1 (MesC-1), 144.4 (CB), 144.9 (C-2,3,6,7), 146.7 (phC-4), 147.7 (PhC-1). Anal. Calcd for $C_{102}H_{82}B_2N_4$ (1385.39): C, 88.43; H, 5.97; N, 4.04. Found: C, 88.14; H, 6.14; N, 3.59.

Crystal Structure Determinations. Data for Cl_4-DBA(Br)$_2$, **5**, **10**, and **20** were collected on a STOE IPDS II two-circle diffractometer with graphite-monochromated Mo K_α radiation (λ = 0.71073 Å). Data for **23**, **26**, **27**, **28**, **31**, **33**, and **35** were collected on a STOE IPDS II two-circle diffractometer with a Genix Microfocus tube with mirror optics using Mo K_α radiation (λ = 0.71073 Å). For Cl_4-DBA(Br)$_2$, **5**, **10**, and **20**, an empirical absorption correction with the program PLATON[56] was performed. The data for **23**, **26**, **27**, **28**, **31**, **33**, and **35** were scaled using the frame scaling procedure in the X-AREA program system.[57] The structures were solved by direct methods using the program SHELXS[58] and refined against F^2 with full-matrix least-squares techniques using the program SHELXL-97.[58]

The Br atom in **5** is disordered over two sites with a site occupation factor of 0.858(3) for the major occupied site.

Both 2-thienyl rings in **23** are disordered over two sites with a site occupation factor of 0.939(8) and 0.727(8), respectively, for the major occupied site. The coordinates and displacement parameters of the overlying S and C atoms were constrained to be equal.

In one molecule of **26**, both 2-thienyl rings are disordered over two sites with a site occupation factor of 0.709(9) and 0.653(7), respectively, for the major occupied site. The coordinates and displacement parameters of the overlying S and C atoms were constrained to be equal.

Both 2-thienyl rings in **28** are disordered over two sites with a site occupation factor of 0.750(4) and 0.538(4), respectively, for the major occupied site. The coordinates and displacement parameters of the overlying S and C atoms were constrained to be equal. The absolute structure was determined (Flack-x-parameter 0.01(9)).

The displacement ellipsoids of all atoms in **31** were restrained to an isotropic behavior. Bond lengths and angles in the chloroform molecules were restrained to be equal. One chloroform molecule was isotropically refined.

CCDC reference numbers: 945733 (Cl_4-DBA$(Br)_2$), 945734 (**5**), 945735 (**10**), 945736 (**20**), 945737 (**23**), 945738 (**26**), 945739 (**27**), 945740 (**28**), 945741 (**31**), 945742 (**33**), 945743 (**35**).

■ ASSOCIATED CONTENT

Ⓢ Supporting Information

Experimental details including assigned NMR data of **7**/**8**, **11**, **12**, **20**/**21**, **28**, **33**, **34**, **35**, and **36**. Experimental details and NMR data of **14**, **15**/**17**, **16**, **18**, and **19** in conjunction with the mechanistic investigation of the DBA formation. X-ray crystal structure analyses of Cl_4-DBA$(Br)_2$, **20**, **27**, **31**, **33**, and **35** and key crystallographic data of Cl_4-DBA$(Br)_2$, **5**, **10**, **20**, **23**, **26**, **27**, **28**, **31**, **33**, and **35**. Cyclic voltammograms of compounds **5**/**6**, **10**, **27**, **29**/**30**, **31**, **33**, **35**, and **36**. Absorption and emission spectra of the compounds **5**/**6**, **10**, **20**−**31**, and **33**−**36** in C_6H_6. Solvatochromism of the compounds **23**−**31**, **35**, and **36**. Mass spectrometric characterization of **36**. ^1H and ^{13}C NMR spectra for the intermediates **14**−**19**. ^1H and ^{13}C NMR spectra in $CDCl_3$ of the new compounds **5**−**13**, **20**−**31**, and **33**−**36**. This material is available free of charge via the Internet at http://pubs.acs.org.

■ AUTHOR INFORMATION

Corresponding Author

matthias.wagner@chemie.uni-frankfurt.de

Notes

The authors declare no competing financial interest.

■ ACKNOWLEDGMENTS

We are grateful to the Sonderforschungsbereich/Transregio 49 project for financial support of this work.

■ REFERENCES

(1) Müller, T. J. J., Bunz, U. H. F., Eds. *Functional Organic Materials: Syntheses, Strategies and Applications*; Wiley-VCH: Weinheim, 2007.

(2) Klauk, H. *Organic Electronics: Materials, Manufacturing and Applications*; Wiley-VCH: Weinheim, 2006.

(3) So, F. *Organic Electronics: Materials, Processing, Devices and Applications*; CRC Press: Boca Raton, FL, 2010.

(4) Müllen, K.; Scherf, U. *Organic Light Emitting Devices: Synthesis, Properties and Applications*; Wiley-VCH: Weinheim, 2006.

(5) Brabec, C.; Scherf, U.; Dyakonov, V. *Organic Photovoltaics - Materials, Device Physics, and Manufacturing Technologies*; Wiley-VCH: Weinheim, 2008.

(6) De Angelis, F.; Gaspari, M.; Procopio, A.; Cuda, G.; Di Fabrizio, E. *Chem. Phys. Lett.* **2009**, *468*, 193−196.

(7) Bénard, C. P.; Geng, Z.; Heuft, M. A.; VanCrey, K.; Fallis, A. G. *J. Org. Chem.* **2007**, *72*, 7229−7236.

(8) Anthony, J. E. *Chem. Rev.* **2006**, *106*, 5028−5048.

(9) Selected reviews: (a) Entwistle, C. D.; Marder, T. B. *Angew. Chem., Int. Ed.* **2002**, *41*, 2927−2931. (b) Entwistle, C. D.; Marder, T. B. *Chem. Mater.* **2004**, *16*, 4574−4585. (c) Jäkle, F. *Coord. Chem. Rev.* **2006**, *250*, 1107−1121. (d) Yamaguchi, S.; Wakamiya, A. *Pure Appl. Chem.* **2006**, *78*, 1413−1424. (e) Matsumi, N.; Chujo, Y. *Polym. J.* **2008**, *40*, 77−89. (f) Elbing, M.; Bazan, G. C. *Angew. Chem., Int. Ed.* **2008**, *47*, 834−838. (g) Jäkle, F. *Chem. Rev.* **2010**, *110*, 3985−4022.

(10) Yu, G.; Yin, S.; Liu, Y.; Chen, J.; Xu, X.; Sun, X.; Ma, D.; Zhan, X.; Peng, Q.; Shuai, Z.; Tang, B.; Zhu, D.; Fang, W.; Luo, Y. *J. Am. Chem. Soc.* **2005**, *127*, 6335−6346.

(11) Shirota, Y.; Kageyama, H. *Chem. Rev.* **2007**, *107*, 953−1010.

(12) Baumgartner, T.; Réau, R. *Chem. Rev.* **2006**, *106*, 4681−4727.

(13) Fichou, D. *Handbook of Oligo- and Polythiophenes*; Wiley-VCH: Weinheim, 1999.

(14) Lorbach, A.; Bolte, M.; Li, H.; Lerner, H.-W.; Holthausen, M. C.; Jäkle, F.; Wagner, M. *Angew. Chem., Int. Ed.* **2009**, *48*, 4584−4588.

(15) Chai, J.; Wang, C.; Jia, L.; Pang, Y.; Graham, M.; Cheng, S. Z. D. *Synth. Met.* **2009**, *159*, 1443−1449.

(16) Lorbach, A.; Bolte, M.; Lerner, H.-W.; Wagner, M. *Chem. Commun.* **2010**, *46*, 3592−3594.

(17) Lorbach, A.; Bolte, M.; Lerner, H.-W.; Wagner, M. *Organometallics* **2010**, *29*, 5762−5765.

(18) Agou, T.; Sekine, M.; Kawashima, T. *Tetrahedron Lett.* **2010**, *51*, 5013−5015.

(19) Januszewski, E.; Lorbach, A.; Grewal, R.; Bolte, M.; Bats, J. W.; Lerner, H.-W.; Wagner, M. *Chem.-Eur. J.* **2011**, *17*, 12696−12705.

(20) Lorbach, A.; Hübner, A.; Wagner, M. *Dalton Trans.* **2012**, *41*, 6048−6063.

(21) Hoffend, C.; Schödel, F.; Bolte, M.; Lerner, H.-W.; Wagner, M. *Chem.-Eur. J.* **2012**, *18*, 15394−15405.

(22) Seven, Ö.; Qu, Z.-W.; Zhu, H.; Bolte, M.; Lerner, H.-W.; Holthausen, M. C.; Wagner, M. *Chem.-Eur. J.* **2012**, *18*, 11284−11295.

(23) Januszewski, E.; Bolte, M.; Lerner, H.-W.; Wagner, M. *Organometallics* **2012**, *31*, 8420−8425.

(24) Zhou, Z.; Wakamiya, A.; Kushida, T.; Yamaguchi, S. *J. Am. Chem. Soc.* **2012**, *134*, 4529−4532.

(25) Hoffend, C.; Diefenbach, M.; Januszewski, E.; Bolte, M.; Lerner, H.-W.; Holthausen, M. C.; Wagner, M. *Dalton Trans.* **2013**, DOI: 10.1039/C3DT51035B.

(26) (a) Yamaguchi, S.; Shirasaka, T.; Akiyama, S.; Tamao, K. *J. Am. Chem. Soc.* **2002**, *124*, 8816−8817. (b) Wakamiya, A.; Mishima, K.; Ekawa, K.; Yamaguchi, S. *Chem. Commun.* **2008**, 579−581. (c) For a 2,3,4,5-tetrakis(2-thienyl)borole, see: Araki, T.; Fukazawa, A.; Yamaguchi, S. *Angew. Chem., Int. Ed.* **2012**, *51*, 5484−5487.

(27) (a) Caruso, A.; Siegler, M. A.; Tovar, J. D. *Angew. Chem., Int. Ed.* **2010**, *49*, 4213−4217. (b) Caruso, A.; Tovar, J. D. *J. Org. Chem.* **2011**, *76*, 2227−2239. (c) Levine, D. R.; Caruso, A.; Siegler, M. A.; Tovar, J. D. *Chem. Commun.* **2012**, *48*, 6256−6258.

(28) Williams, V. C.; Dai, C.; Li, Z.; Collins, S.; Piers, W. E.; Clegg, W.; Elsegood, M. R. J.; Marder, T. B. *Angew. Chem., Int. Ed.* **1999**, *38*, 3695−3698.

(29) Chen, J.; Kampf, J. W.; Ashe, A. J., III. *Organometallics* **2008**, *27*, 3639−3641.

(30) Dou, C.; Saito, S.; Matsuo, K.; Hisaki, I.; Yamaguchi, S. *Angew. Chem., Int. Ed.* **2012**, *51*, 12206−12210.

(31) Lorbach, A.; Reus, C.; Bolte, M.; Lerner, H.-W.; Wagner, M. *Adv. Synth. Catal.* **2010**, *352*, 3443−3449.

(32) Reus, C.; Liu, N.-W.; Bolte, M.; Lerner, H.-W.; Wagner, M. *J. Org. Chem.* **2012**, *77*, 3518−3523.

(33) Both in C_6D_{12} and in C_6D_6 we detected traces of: (i) 1-bromo-3-trimethylsilylbenzene: Stehouwer, J. S.; Jarkas, N.; Zeng, F.; Voll, R. J.; Williams, L.; Owens, M. J.; Votaw, J. R.; Goodman, M. M. *J. Med. Chem.* **2006**, *49*, 6760−6767. (ii) 1-Bromo-3,5-bis(trimethylsilyl)-benzene: Beinhoff, M.; Karakaya, B.; Schlüter, A. D. *Synthesis* **2003**, 79−90. These appeared already 1 h after the sample had been prepared but did not increase significantly in amount with time.

We therefore assume that these compounds are primarily formed by the reaction of **3** with small quantities of HBr present in BBr_3: Seyferth, D.; White, D. L. *J. Am. Chem. Soc.* **1972**, *94*, 3132−3138. At high temperatures and in the presence of excess BBr_3, 1-bromo-3-trimethylsilylbenzene and 1-bromo-3,5-bis(trimethylsilyl)benzene are finally transformed into 1-bromo-3-dibromoborylbenzene and 1-bromo-3,5-bis(dibromoboryl)benzene.

(34) (a) Bruice, P. Y. *Organic Chemistry*, 5th ed.; Pearson Education, Inc.: NJ, 2007. (b) Roberts, J. D.; Sanford, J. K.; Sixma, F. L. J.; Cerfontain, H.; Zagt, R. *J. Am. Chem. Soc.* **1954**, *76*, 4525−4534. (c) Coombes, R. G.; Crout, D. H. G.; Hoggett, J. G.; Moodie, R. B.; Schofield, K. *J. Chem. Soc. B* **1970**, 347−357.

(35) Kaufmann, D. *Chem. Ber.* **1987**, *120*, 901−905.

(36) A related thermal rearrangement reaction has been reported for 1-trimethylstannyl-2-dichloroborylferrocene: (a) Jäkle, F.; Lough, A. J.; Manners, I. *Chem. Commun.* **1999**, 453−454. (b) Gamboa, J. A.; Sundararaman, A.; Kakalis, L.; Lough, A. J.; Jäkle, F. *Organometallics* **2002**, *21*, 4169−4181.

(37) (a) Muetterties, E. L. *J. Am. Chem. Soc.* **1959**, *81*, 2597. (b) Muetterties, E. L. *J. Am. Chem. Soc.* **1960**, *82*, 4163−4166. (c) Kölle, P.; Nöth, H. *Chem. Rev.* **1985**, *85*, 399−418. (d) Piers, W. E.; Bourke, S. C.; Conroy, K. D. *Angew. Chem., Int. Ed.* **2005**, *44*, 5016−5036. (e) De Vries, T. S.; Prokofjevs, A.; Vedejs, E. *Chem. Rev.* **2012**, *112*, 4246−4282. (f) Bagutski, V.; Del Grosso, A.; Carrillo, J. A.; Cade, I. A.; Helm, M. D.; Lawson, J. R.; Singleton, P. J.; Solomon, S. A.; Marcelli, T.; Ingleson, M. J. *J. Am. Chem. Soc.* **2013**, *135*, 474−487.

(38) Ishida, N.; Moriya, T.; Goya, T.; Murakami, M. *J. Org. Chem.* **2010**, *75*, 8709−8712.

(39) See ref 36b and also: Boshra, R.; Venkatasubbaiah, K.; Doshi, A.; Lalancette, R. A.; Kakalis, L.; Jäkle, F. *Inorg. Chem.* **2007**, *46*, 10174−10186.

(40) Wang, N.; Hudson, Z. M.; Wang, S. *Organometallics* **2010**, *29*, 4007−4011.

(41) These substituents have already been employed for the development of donor−acceptor−donor triads featuring 9-borafluorene or dibenzo[*b*,*f*]borepin acceptors. See refs 26 and 27b.

(42) Compounds related to **33**−**36** have appeared in the recent patent literature as materials for organic electroluminescence devices: (a) Meng, A. PCT Int. Appl. WO 2006/050496, 2006. (b) Stoessel, P.; Heil, H.; Parham, A.; Vestweber, H. DE 10 2006/013802, 2006.

(43) Yang, C.; Jacob, J.; Müllen, K. *Macromol. Chem. Phys.* **2006**, *207*, 1107−1115.

(44) (a) Karplus, M.; Pople, J. A. *J. Chem. Phys.* **1963**, *38*, 2803−2807. (b) Günther, H.; Schmickler, H.; Königshofen, H.; Recker, K.; Vogel, E. *Angew. Chem., Int. Ed.* **1973**, *12*, 243−245. (c) Levin, R. H.; Roberts, J. D. *Tetrahedron Lett.* **1973**, *14*, 135−138. (d) Farnum, D. G. *Adv. Phys. Org. Chem.* **1975**, *11*, 123−175.

(45) Bock, B.; Kuhr, M.; Musso, H. *Chem. Ber.* **1976**, *109*, 1184−1194.

(46) Iida, A.; Sekioka, A.; Yamaguchi, S. *Chem. Sci.* **2012**, *3*, 1461−1466.

(47) Braunschweig, H.; Dyakonov, V.; Jimenez-Halla, J. O. C.; Kraft, K.; Krummenacher, I.; Radacki, K.; Sperlich, A.; Wahler, J. *Angew. Chem., Int. Ed.* **2012**, *51*, 2977−2980.

(48) Mercier, L. G.; Piers, W. E.; Parvez, M. *Angew. Chem., Int. Ed.* **2009**, *48*, 6108−6111.

(49) The inseparable compound mixtures **5**/**6**, **20**/**21**, and **29**/**30** have been included into the investigation of optoelectronic properties. We are aware of the fact that an uncritical use of data obtained on compound mixtures might give misleading results. However, a comparison of the optoelectronic properties of pure **23** with those of the isomeric mixture **23**/**24** revealed essentially no differences. Any discussion of data obtained on **5**/**6**, **20**/**21**, and **29**/**30** is based on the working hypothesis that the same would be true also in these cases. Related investigations of photophysical properties of isomeric mixtures of 2,9- and 2,10-substituted pentacenes can be found in the literature: Yamada, H.; Yamashita, Y.; Kikuchi, M.; Watanabe, H.; Okujima, T.; Uno, H.; Ogawa, T.; Ohara, K.; Ono, N. *Chem.-Eur. J.* **2005**, *11*, 6212−6220.

(50) Lakowicz, J. R. *Principles of Fluorescence Spectroscopy*, 3rd ed.; Springer: New York, 2006. The band gap values were calculated from the onset wavelength (λ_{onset}) of the absorption spectra.

(51) Dawson, W. R.; Windsor, M. W. *J. Phys. Chem.* **1968**, *72*, 3251−3260.

(52) Morris, J. V.; Mahaney, M. A.; Huber, J. R. *J. Phys. Chem.* **1976**, *80*, 969−974.

(53) Anthony, J. E. *Chem. Rev.* **2006**, *106*, 5028−5048.

(54) For the determination of the quantum yields of thin films, at least four films of varying thicknesses were generated for each compound by evaporation of differently concentrated samples in $CHCl_3$ at 100 °C on a quartz-glass surface. Using this experimental setup and an integrating sphere system, the measured solid-state quantum yield of a thin film of the standard green OLED material tris(8-hydroxyquinoline)aluminum (Alq_3) is in line with the published value (estimated error margin ± 10%): (a) Cölle, M.; Gmeiner, J.; Milius, W.; Hillebrecht, H.; Brütting, W. *Adv. Funct. Mater.* **2003**, *13*, 108−112. (b) Kumar, N. S. S.; Varghese, S.; Rath, N. P.; Das, S. *J. Phys. Chem. C* **2008**, *112*, 8429−8437.

(55) Ref 26b.

(56) Spek, A. L. *J. Appl. Crystallogr.* **2003**, *36*, 7−13.

(57) Stoe & Cie. *X-AREA. Diffractometer control program system*; Stoe & Cie: Darmstadt, Germany, 2002.

(58) Sheldrick, G. M. *Acta Crystallogr., Sect. A* **2008**, *64*, 112−122.